

DeepSight: Mitigating Backdoor Attacks in Federated Learning Through Deep Model Inspection

Phillip Rieger, Thien Duc Nguyen, Markus Miettinen, Ahmad-Reza Sadeghi

Technical University of Darmstadt, Germany

{phillip.rieger, duchtien.nguyen, markus.miettinen, ahmad.sadeghi}@trust.tu-darmstadt.de

Abstract—Federated Learning (FL) allows multiple clients to collaboratively train a Neural Network (NN) model on their private data without revealing the data. Recently, several targeted poisoning attacks against FL have been introduced. These attacks inject a backdoor into the resulting model that allows adversary-controlled inputs to be misclassified. Existing countermeasures against backdoor attacks are inefficient and often merely aim to exclude deviating models from the aggregation. However, this approach also removes benign models of clients with deviating data distributions, causing the aggregated model to perform poorly for such clients.

To address this problem, we propose *DeepSight*, a novel model filtering approach for mitigating backdoor attacks. It is based on three novel techniques that allow to characterize the distribution of data used to train model updates and seek to measure fine-grained differences in the internal structure and outputs of NNs. Using these techniques, *DeepSight* can identify suspicious model updates. We also develop a scheme that can accurately cluster model updates. Combining the results of both components, *DeepSight* is able to identify and eliminate model clusters containing poisoned models with high attack impact. We also show that the backdoor contributions of possibly undetected poisoned models can be effectively mitigated with existing weight clipping-based defenses. We evaluate the performance and effectiveness of *DeepSight* and show that it can mitigate state-of-the-art backdoor attacks with a negligible impact on the model’s performance on benign data.

Keywords – *Deep Learning (DL), Federated Learning (FL), Poisoning, Backdoor, Model Inspection*

I. INTRODUCTION

Federated Learning (FL) enables multiple clients to collaboratively train a Neural Network (NN) model. This is done by an iterative process in which clients train their models locally using their own data and send only trained model updates to a central server, which aggregates them and distributes the resulting global model back to all clients. The federated approach promises clients to keep their training data private and the server to reduce the computational costs as the model training is parallelized and outsourced to the clients. These benefits make FL highly useful, especially in applications with privacy-sensitive data such as medical image recognition [33], word suggestion systems on smartphone keyboards (Natural Language Processing; NLP) [22], or network intrusion detection systems (NIDS) [26].

Backdoor Attacks. On the other hand, the server cannot control the training process of the participating clients. An adversary can compromise a subset of the clients and use them to inject a backdoor into the aggregated model. In the examples above the adversary’s goal would be to cause the aggregated model to classify malware network traffic patterns as benign to avoid detection by the NIDS, or in the case of NLP to manipulate the text prediction model to propose specific brand names to inconspicuously advertise them¹. Recently, various attack strategies for targeted poisoning, so-called *backdoor* attacks, have been proposed utilizing compromised clients to submit poisoned model updates [2], [27], [34], [41], [38].

Problems of Existing Backdoor Defenses. The currently proposed mitigations against backdoor attacks follow two main strategies: (1) aim to detect and remove poisoned models [34], [4], [24], [28] and (2) aim to limit their impact, e.g., by restricting the L_2 -norm of updates (called clipping) [2], [28], [23], [10]. In the first strategy, model updates differing from the majority are considered suspicious and excluded from aggregation. However, those approaches cannot distinguish between models that were trained on benign training data with different data distributions and poisoned models. This causes performance degradation of the resulting model, as this strategy will not only reject poisoned model updates but also deviating benign model updates. Moreover, these defenses fail in dynamic attack scenarios (cf. §II-B2 and App. B). The second defense strategy has the drawback that it is not effective against poisoned model updates with high attack impact. For example, when adding training samples for the backdoor behavior to the original (benign) training data, the poisoned model achieves higher accuracy on the backdoor task.

Adversarial Dilemma: The adversary can arbitrarily choose its attack strategy: On one hand, it can use a high ratio of poisoned data for training the backdoor task. However, this causes the poisoned models to differ from benign models, making the poisoned models easy to detect by a filtering-based defense. On the other hand, if the adversary does not follow this strategy, the attack can be easily mitigated by any defense that limits the impact of the individual models as the poisoned models are outnumbered by benign models (cf. §II-C for details). Combining both defense strategies, therefore, creates a dilemma for the adversary: Either the attack is filtered by one part of the defense or the other part makes the impact of the attack negligible [28].

Unfortunately, a naïve combination of both defense strategies is not effective, as existing filtering mechanisms follow an

¹Especially systems with a large user base are attractive for such attacks, e.g., the FL-based keyboard input suggestion system GBoard [22] has been downloaded more than 1 billion times [11]

outlier-detection strategy [34], [4], [24], [28] that also filters benign models with deviating data distributions. Consequently, a high number of clients are wrongly excluded leading to performance degradation of the aggregated model for their data.

Our Approach: To address these problems, we propose DeepSight, a novel model filtering approach that deeply inspects the internal structure and outputs of the NNs for identifying malicious model updates with high attack impact while keeping benign model updates, even if these originate from clients with deviating data distributions. By combining our novel filtering scheme with clipping we exploit the above-mentioned adversarial dilemma to ensure that the adversary’s strategy focuses the training on the backdoor task. This, on the other hand, causes the structure of the resulting NN to contain artifacts related to this backdoor.

We propose several techniques to analyze the internal structure of model updates for identifying characteristics of the training data distribution and to measure fine-grained differences between the models. Based on these techniques, we develop an approach to identify models trained with a data distribution focusing on a specific task (the backdoor task) and also to group models together that were trained on similar data. Those techniques enable our approach to reliably identify model clusters that with a high likelihood contain poisoned models and consequently exclude them from aggregation. Our extensive evaluation shows that our approach mitigates recent state-of-the-art backdoor attacks [2], [27], [41]. We show that DeepSight filters model updates with high attack impact so that possibly remaining poisoned model updates will be effectively mitigated using existing clipping defenses, while the benign training process is not affected by wrongly excluded benign models. Our contributions include:

- We propose DeepSight, a novel defense to mitigate targeted poisoning (backdoor) attacks on Federated Learning (FL). DeepSight uses a novel filtering scheme that conducts a deep model inspection and combines it with clipping (§V) to identify targeted poisoning attacks.
- We propose a voting-based model filtering scheme combining a classifier and clustering-based similarity estimations. The individual labels are used to *reliably identify clusters with malicious model updates*, such that not only a model’s label is used but also the labels of similar models for deciding on accepting or rejecting a model update (§V-A4). Together with the classifier as the central mechanism, instead of an outlier elimination-based strategy, we prevent models of benign clients with deviating data distributions from being filtered out, thereby increasing the performance of the aggregated model for the data of these clients.
- We propose the Threshold Exceedings metric (§IV) that analyzes the parameter updates of the output layer for a model to *measure the homogeneity of its training data*. We use this metric to build a classifier, being capable of labeling model updates as benign or suspicious.
- We design an ensemble of clustering algorithms, based on three different techniques to effectively identify and cluster model updates with similar training data (§V-A3) to support the classifier by similarity estimations.
- We propose two novel *techniques for measuring fine-grained differences in the structure and outputs of NNs* (§IV): The first technique Division Differences (DDifs)

focuses on changes in model prediction outputs while the second technique Normalized Update Energies (NEUPs) measures changes in parameter updates for the output layer of the NN. To the best of our knowledge, this is the first work that uses a deep analysis of the models, their predictions, and individual neurons for mitigating poisoning attacks in Federated Learning (FL).

- We extensively evaluate the performance and effectiveness of DeepSight (§VI). We show that our defense mechanism does not affect the performance of the resulting model. For showing DeepSight’s effectiveness we evaluated several state-of-the-art backdoor attacks [2], [27], [41], [38].
- As a side effect, we demonstrate a successful backdoor attack on a recently proposed ‘provably-secure’ FL backdoor defense [6] (§VI-C1). We will discuss that the theoretical proof includes a-posteriori knowledge, making assumptions that do not hold in practice. However, DeepSight is able to mitigate such attacks (§VIII).

II. BACKGROUND

A. Federated Learning

McMahan *et al.* [21] introduced Federated Learning (FL) as a process that leverages many different clients for collaboratively training a machine learning model, here a Neural Network (NN), based on their local datasets. In contrast to a centralized approach, the local data of each client never leaves this client, allowing the clients to keep their data secret.

Each round t of an FL process consists of the following steps: **Step 1:** Each client $k \in \{1, \dots, N\}$, trains locally a ML model on its private data, starting from the global G_t before sending its model update to a central aggregation server S .

Step 2: The server merges the received updates and applies the aggregated update on the global model.

Step 3: The resulting model, called aggregated model G_{t+1} , is distributed back to all participants.

Different aggregation rules have been proposed, e.g., Federated Averaging (FedAvg) [21], Krum [4], or Trimmed Mean [42]. Although we will evaluate our proposed defense also for other aggregation rules, e.g., for Krum [4], we will focus on FedAvg as it is widely used in FL [26], [5], in particular in work about backdoor attacks [2], [27], [34], [24], [28], [10].

In FedAvg, the aggregated model G_{t+1} is determined by averaging all received model updates and adding it to the previous global model G_t . Although this algorithm also allows weighting the contributions of different clients, e.g., to increase the impact of clients with a large training dataset, this also makes the system more vulnerable for manipulations, as compromised clients could exploit this, e.g., by lying about their dataset sizes to increase their impact. Therefore, we follow existing work [2], [34], [4], [28], [10], [21] and weight all model updates equally.

B. Backdoor Attacks on FL

In a targeted poisoning attack, also called backdoor attack, an adversary \mathcal{A} manipulates the local models of a subset of clients with size $N_{\mathcal{A}}$ (cf. §III). Its goal is, to make the aggregated model that is operated on a feature space \mathcal{D} output a certain class $C_{\mathcal{A}}$ for a set of input samples, called trigger set $\mathcal{I} \subset \mathcal{D}$. The success of the attack is determined by

the Backdoor Accuracy (BA), which measures the accuracy for the backdoor task. For example, in a word prediction scenario, the backdoor could be to predict the word "delicious" after the trigger sentence "pasta from astoria tastes" [2]. The BA indicates here, for how many occurrences of the trigger sentence the model suggests "delicious". The ratio of compromised clients to the total number of clients will be denoted as Poisoned-Model-Rate (PMR). For backdoor attacks, widely two attack strategies are considered by previous work, assuming different thread models.

1) *Data Poisoning*: In the weaker adversary model, \mathcal{A} is restricted to manipulating the training data of a client. \mathcal{A} poisons the client's training data by adding malicious attack data to the dataset. The attack data consists of input samples from the trigger set, with the new, adversary-chosen (wrong) label $C_{\mathcal{A}}$. For example, in the NIDS scenario, \mathcal{A} can achieve this by creating malware traffic during the NIDS system captures network packets that will be used as benign training data [27]. However, \mathcal{A} still needs to ensure that the resulting model updates are not too conspicuous, e.g., by limiting the Poisoned-Data-Rate (PDR), i.e., the fraction of attack data injected into the training dataset. By choosing a suitable PDR, \mathcal{A} can balance between attack impact and attack stealthiness. Let D_i denote the benign dataset of a compromised client i and $D_i^{\mathcal{A}}$ the injected attack data, then the PDR of the combined, poisoned dataset D_i' is given by:

$$\text{PDR} = \frac{|D_i^{\mathcal{A}}|}{|D_i'|} \quad (1)$$

The advantage of this attack is that it is sufficient to poison the dataset, which can be done, without compromising the client that actually trains the NN. Therefore, it requires fewer capabilities of \mathcal{A} , compared to the Model Poisoning attack.

2) *Model Poisoning*: In a stronger adversary model \mathcal{A} is able to compromise a subset of the clients and fully control them. \mathcal{A} can then change the model updates arbitrarily before submitting them to increase attack impact on the aggregated model. This allows \mathcal{A} to adapt the training algorithm, its parameters, and to scale model updates to increase the attack impact without triggering defense mechanisms that may be deployed on the aggregation server [2]. If the adversary has full control over a client, it can also arbitrarily change their behavior, e.g., using a subset of clients for random updates to distract the defense mechanism (cf. App. B). The model poisoning attack can be split into two parts:

Scaling: As proposed by Bagdasaryan *et al.* [2], \mathcal{A} can scale the differences between the (poisoned) trained model $W_{t,i}^*$ of the client i in round t and the used global model G_t , before submitting the model. This up-scaling increases the impact of the poisoned models during the aggregation. If there are N clients in total, from which $N_{\mathcal{A}}$ are compromised, \mathcal{A} can scale the updates using a factor up to $N/N_{\mathcal{A}}$.

To circumvent deployed defense mechanisms \mathcal{A} can restrict the L_2 -norm for the update to a chosen value S . This prevents the scaled updates from being too suspicious to the cost of the impact of the attack. The scaling factor $\gamma_{t,i}$ of a compromised client i in round t is, therefore, given by:

$$\gamma_{t,i} = \max \left(1, \min \left(\frac{N}{N_{\mathcal{A}}}, \frac{S}{\|W_{t,i}^* - G_t\|} \right) \right) \quad (2)$$

The scaled malicious model $W'_{t,i}$ is then given by:

$$W'_{t,i} = (W_{t,i}^* - G_t) \gamma_{t,i} + G_t \quad (3)$$

Anomaly-Evasion As scaling makes the model update more suspicious, Bagdasaryan *et al.* [2] proposed to reduce the learning rate of the clients. Furthermore, they adapted the loss function to make the model more inconspicuous by adding a term L_{anomaly} that measures the similarity between the original model and the used global model, e.g., by using their cosine distance. If the normal loss function L_{class} measures the performance of the model on the actual task and the loss-control parameter α weights the impact of both parts, then the adapted loss function L' is given by:

$$L' = \alpha L_{\text{class}} + (1 - \alpha) L_{\text{anomaly}} \quad (4)$$

In the rest of the paper, we will use the strong adversary model, where \mathcal{A} uses a combination of the Anomaly-Evasion and Scaling attack strategies, called *constrain-and-scale* attack [2].

C. Exploiting Adversary's Dilemma

Adversary \mathcal{A} can freely choose an attack strategy that is most effective for it. It can either use well-trained poisoned models to inject the backdoor, e.g., by using a high PDR, or, train the models only weakly, e.g., by using a low PDR. However, as pointed out by Nguyen *et al.* [28], well-trained models differ significantly from benign models and are, therefore, easy to detect by approaches that filter suspicious models. On the other hand, the impact of weakly trained models is likely to become negligible during aggregation, as poisoned models are outnumbered by benign ones [28]. Bagdasaryan *et al.* proposed scaling the updates to increase their contribution to the aggregated model [2]. However, this attack is easy to mitigate by approaches that limit the contribution of the individual clients, e.g., clipping that limits the L_2 -norm of the model updates.

III. SYSTEM AND PROBLEM SETTING

A. System Setting

We consider a system with N clients that train their local models before sending them to the aggregator \mathcal{S} who combines them by using FedAvg [21]. We assume that clients keep their data secret. Therefore, no training or testing data is available on the aggregation server \mathcal{S} .

We also assume that the data of different clients may differ from each other. Without loss of generality, the individual clients can be seen as parts of groups of clients with similar training data, s.t. the data of all clients in the same group follows the same distribution, therefore, are IID. There can be one or multiple groups of arbitrary, also different sizes (also with size one). Taking the NLP scenario as an example, if people write similar texts, e.g., always about the same topic, also the updates for the NN that is used for the word suggestion will be similar. Therefore, the model updates of those clients can be seen as a group of updates with similar, IID training data. Other users may write about another topic, such that their model updates can be seen as a different group. If all people would write about the same topic, their model updates can be seen as one (big) group and if a single person writes very unique texts, e.g., by using very

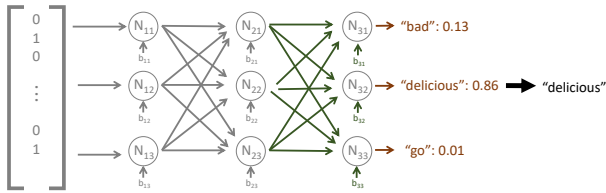


Fig. 1: Structure of a simplified NN for word suggestion. The individual colors refer to the parameters that are used by the proposed techniques

special words, the respective model update can be seen as part of a group having only one member.

The techniques that we propose later (cf. §IV), allow characterizing the clients’ training data to make these groups visible. This allows clustering the received model updates accordingly to support the classifier.

B. Adversary Model

In the rest of the paper, we consider an adversary \mathcal{A} that aims to inject a backdoor into the aggregated model, making the model predict a certain label $C_{\mathcal{A}}$ for some specific, adversary-controlled input samples, called trigger set \mathcal{I} . The manipulated aggregated model shall then be distributed to all clients.

However, if the aggregator \mathcal{S} notices the attack it will exclude the poisoned models. If \mathcal{S} notices the attack but cannot identify the poisoned models, it can repeat the training with different subsets of clients until no attack is detected [3]. Hence, the attack also must not degrade the performance of the aggregated model on the main task (Main Task Accuracy, MA).

Formally, if G_t is the aggregated model after the attack, G_{t-1} the global model before the attack, \mathcal{D} the set of all possible inputs, $\mathcal{I} \subset \mathcal{D}$ the trigger set and $f(G_t, x)$ the prediction of the model G_t on the input sample $x \in \mathcal{D}$, \mathcal{A} ’s goal is:

$$\forall x^* \in \mathcal{I}. f(G_t, x^*) = C_{\mathcal{A}} \wedge \forall x \in \mathcal{D} \setminus \mathcal{I}. f(G_t, x) = f(G_{t-1}, x) \quad (5)$$

Therefore, from Eq. 5, two objectives for \mathcal{A} can be derived:

O1: Performance on the backdoor task. The aggregated model shall predict $C_{\mathcal{A}}$ for triggered samples.

O2: Stealthiness. \mathcal{A} must ensure that the poisoned models are inconspicuous to \mathcal{S} and that \mathcal{S} cannot determine, whether a poisoning attack took place. This includes preventing a drop in the MA.

Aligned with the existing work on backdoor attacks [2], [27], [34], [4], [24], [28], we consider a strong adversary model, allowing \mathcal{A} to fully control $N_{\mathcal{A}} < N/2$ clients. However, \mathcal{A} has no control over the benign clients nor has access to their data or model updates. We assume \mathcal{A} to have full knowledge of the aggregation server \mathcal{S} and any deployed defense, i.e., used algorithms and configuration parameters, however, \mathcal{A} cannot tamper with it.

C. Objectives of a Poisoning Defense

To defeat the objectives of the adversary, the defense has to fulfill the following security requirement:

R1: Poisoning Mitigation. The defense must mitigate the poisoning attack. Therefore, the BA must remain at the same level as without the attack ². However, as already pointed out

²It worth to note that for some backdoor tasks, misclassification of the model are counted in favor of the BA, s.t., the BA is higher than 0 %, even without attack (cf. App. F).

in §I, it is not sufficient for defenses to mitigate poisoning attacks, but also satisfy certain requirements such as model performance. Therefore, we consider defense against poisoning attacks only effective if it also fulfills the following additional requirements:

R2: No Disruption of the Training Process. The defense should not negatively affect the training. Therefore, the performance of the resulting model on the main task (Main Task Accuracy, MA) must be at the same level as without defense.

R3: Autonomous Process The defense must run fully autonomous, i.e., no manual configuration nor any knowledge, e.g., estimations for the L_2 -norms of benign updates or validation data³, must be required.

To the best of our knowledge, all existing approaches for identifying poisoned updates are based on metrics that consider the NN as a black box, e.g., cosine [24], [28], [10] or L_2 -norm [4]. Our novel scheme, therefore, addresses the following challenges:

C1: How to distinguish poisoned models from benign models that were trained on different data.

C2: How to entangle to the backdoor performance such that the only way for \mathcal{A} to bypass a scheme that is based on these techniques is to reduce the backdoor performance.

C3: How to make the techniques generally applicable, without knowing the exact data. For example, for the NIDS scenario, it should not make a difference, whether the models analyze the network traffic of IP cameras or smart sensors.

C4: How to ensure a high precision, to prevent benign models from being excluded wrongly.

C5: How to effectively combine the individual techniques to a dynamic defense scheme, s.t. it can dynamically adapt to attacks. Therefore, neither the scheme shall be broken unless \mathcal{A} overcomes every single technique, nor shall the scheme suffer by false positives.

D. Proposed Techniques

Figure 1 shows a simplified, linear NN for suggesting words based on the previously typed text. The NN has 3 layers with 3 neurons each. The arrows that connect the neurons represent the respective weights, $b_{i,k}$ the bias for the respective neuron, and the brown number the calculated scores. In this example, the NN suggests ”delicious” as the next word, since it has the highest score.

We propose 3 techniques that allow to analyze NNs and provide characteristics about the distribution of the used training data. The first technique is called Division-Difference (DDif). When training a NN, the predicted score for the current sample (e.g., ”pasta from astoria tastes **delicious**”) is increased. However as a side-effect, also the score (colored brown in Fig. 1) for the current label, i.e., ”delicious” is increased in general, therefore, also when another input is used. The DDifs measures these changes as they provide information about the distribution of the training labels of the respective client.

When training a NN, the respective weights are adapted slightly for each sample in order to increase the predicted score. Since each neuron in the last layer of a NN represents

³For example, in the case of the FL-based NIDS DfIoT [26], new training processes for new data scenarios is started automatically. Therefore, neither validation data nor prior knowledge about the model updates like their L_2 -norms are available as this would require the clients to share their data, which would violate a principal design goal of FL.

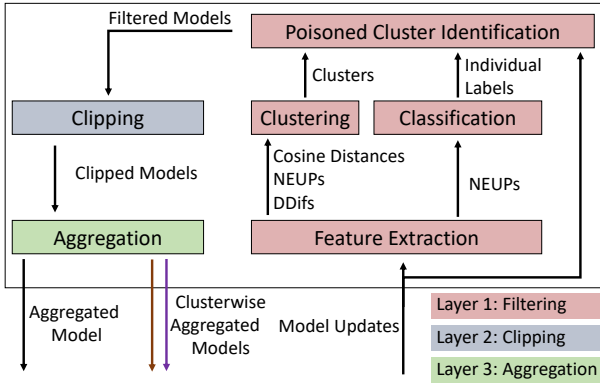


Fig. 2: Structure of DeepSight

an output label, the total magnitude of changes for the parameters of the individual neurons (colored in green in Fig. 1) is connected to the frequency of the individual labels. The Normalized Update energies (NEUPs) measure those changes and use them to provide a rough estimation of the output labels for the training data of the individual clients.

The task of a backdoor is usually very simple compared to the benign task of a model. For example, in case of the NLP scenario, instead of learning a large number of different sentences, the backdoor task consists only of predicting the correct word after a specific sentence, i.e., "pasta from astoria tastes **delicious**". To prevent, that the impact of the attack becomes negligible during the evaluation \mathcal{A} needs to use a high PDR (cf. II-C), resulting in a focus of the labels on the target word, i.e., "delicious". For example, in case of a PDR of 50% half of the labels belongs to those 5 words, although there are 50 000 words in total (cf. §VI-A1). The Threshold Exceedings uses the NEUPs to compare the distribution of labels for measuring the homogeneity of labels in the training data. The classifier in the proposed filtering scheme analyses the homogeneity value for each model. If a model update has a strong focus in the used training data, therefore, if few labels occur with a significantly higher frequency than all other labels, then the classifier considers this update as poisoned.

E. Our Defense Approach

We propose DeepSight, an effective novel filtering approach against dynamic backdoor attacks that overcomes the deficiencies of previous work. Its overall structure is shown in Fig. 2. DeepSight uses a classifier as the central component that is based on deep-model-inspection (cf. §V-A). The filtering is followed by a weight clipping component (cf. §V-B), which enforces \mathcal{A} 's strategy to focus the training data of poisoned models on the backdoor behavior. Otherwise, the attack can either be mitigated by the clipping layer (cf. §V-B) or its impact becomes negligible in the aggregation phase (cf. §V-C). The first layer of the defense realizes a classification-based filtering and removes poisoned models with high attack impact, where the training data is focused on samples for the backdoor behavior. Here, we design an algorithm to combine the different techniques, s.t., the classification is supported by the similarity estimations, without following an outlier-detection-based approach like existing approaches that use clustering. The filtering scheme is based on the proposed novel techniques for measuring fine-grained differences between the structure and outputs of a model and uses them to deeply analyze the

individual models, taking into account their predictions, individual neurons as well as an estimation for the homogeneity of the used training data. The subsequent layers (clipping and aggregation) mitigate the effect of potentially remaining, weakly-trained poisoned models. The structure of DeepSight is shown in Fig. 2. The filtering layer performs three major steps:

- 1. Classification** DeepSight utilizes a novel metric entitled *Threshold Exceedings* that measures the homogeneity of a model's training data to label models as benign or suspicious.
- 2. Clustering** Secondly, DeepSight groups model updates, such that all models in the same group have been trained on similar training datasets. Therefore, this component clusters the models according to the groups of clients with IID data that were discussed in §III-A. This allows DeepSight to reliably separate malicious and benign model updates into different clusters and, therefore, support the labeling by similarity estimations. DeepSight uses two additional novel techniques *Division Differences (DDifs)* and *Normalized Energy Updates (NEUPs)* that enable it to extract characteristics of a model's training data as well as the cosine metric.
- 3. Poisoned Cluster Identification** In the last filtering step, the labeling and the clustering are combined to discriminate clusters containing poisoned models and for finally deciding about excluding or accepting each model update.

IV. TECHNIQUES FOR ANALYZING ML MODELS' TRAINING DATA DISTRIBUTIONS

In this section we introduce several novel techniques for deep inspection and analysis of model updates to identify models whose training data were focused on a specific (backdoor) task and measure fine-grained differences between models. In §V we will describe how the filtering component and in particular the classifier of DeepSight is based on these techniques.

We introduce *Division Differences (DDifs)* that measures the difference between the predicted scores of the local and global models. As all clients use the same global model, in case of similar or different training data, also the predicted probabilities will change accordingly. Therefore, they provide information about the distribution of labels in the training data. Moreover, we introduce *NEUPs*, which analyze the total magnitude of the updates for the individual neurons of the output layer. NEUPs use these magnitudes to determine a rough estimation of the distribution of labels in the training data of the model update, allowing, e.g., to measure the similarity of the training data for different model updates.

The third technique, entitled *Threshold Exceedings*, uses NEUPs for measuring the homogeneity of labels in the used training data. In §V-A, we describe how Threshold Exceedings are used to identify models as benign or poisoned.

A. Division Differences

When training a NN, each specific sample consists of an input x and an output category y . During the training, the parameters of the NN are adjusted iteratively, s.t. the score for y that is predicted by the current model for x is maximized. For example, in the NLP scenario x could be a sequence of words and y the suggested next word. However, this has the side effect that also for another input x^* , with a different label y^* , the score that is predicted for y also changes very slightly, although $y \neq y^*$. This phenomenon occurs especially when samples of the category y occur very frequently in the

training data. However, because of using clipping as part of the defense, \mathcal{A} has to use a high PDR, causing the target category of the backdoor, e.g., in case of the NLP scenario, the word "delicious", to occur very frequently. Therefore, especially for backdoor samples, the probability of the target label is increased in general and not only for samples of this category [18]. In the following, we will exploit this by comparing the probabilities that were predicted by a local model $W_{t,k}$ to the predicted probabilities of the used global model G_t . The rationale here is that if two models $W_{t,i}$ and $W_{t,k}$ were trained on similar data, also the ratios of their probabilities compared to the predictions of the global model will be similar. The information that is gained by this technique allows identifying clients with similar training data. We will refer to this technique as *Division Differences* (DDifs).

Because all clients start from the same global model and clients with similar data will try to achieve similar predictions for their data samples, they will adapt their parameters similarly, resulting in similar model updates. For example, considering a NN with n output classes, e.g., the number of known words in the NLP scenario, a specific sample x , 2 clients k and l with similar data, their respective local models in round t $W_{t,k}$ and $W_{t,l}$, then their predictions $f(x; W_{t,k}), f(x; W_{t,l}) \in \mathcal{R}^n$ will be also very close. It follows directly that when comparing those predictions to the predictions of the original model $f(x; G_t)$, the differences between $f(x; W_{t,k})$ and $f(x; G_t)$ as well as $f(x; W_{t,l})$ and $f(x; G_t)$ provides information about the similarity of the training data of k and l .

A problem is that the server has no input data for evaluating the NNs, as we assume that the server has neither training nor testing data (cf. §III-A). We solve this problem by using random input vectors instead of actual data. As we focus on the differences between predictions of the global model G_t and the predictions of the local model $W_{t,k}$ of each client k rather than finding the class with the highest predicted probability, it is not necessary to obtain meaningful predictions. Therefore, it is not necessary to use real data samples. The rationale is that for a poisoned model update W' the predicted probabilities for the backdoor target class will be increased in general (cf. Liu *et al.* [18]), independently from the actual input, and, therefore also show corresponding differences in comparison to the predictions of the preceding global model G_t .

For calculating the DDifs for a model update $W_{t,k}$ of client k during training iteration t , we generate $N_{\text{samples}} = 20\,000$ random input samples s_m ($m \in [0, N_{\text{samples}} - 1]$) and provide them as input to model $W_{t,k}$. We then divide the probabilities $f(s_m; W_{t,k})_i$ predicted by the local model for each output neuron i by the corresponding neuron-specific prediction $f(s_m; G_t)_i$ of the global model G_t :

$$\text{DDif}_{t,k,i} = \frac{1}{N_{\text{samples}}} \sum_{m=1}^{N_{\text{samples}}} \frac{f(s_m; W_{t,k})_i}{f(s_m; G_t)_i} \quad (6)$$

B. Normalized Update Energy

The second measure that we propose for identifying clients with similar training data is the NormalizEd UPdate energy (NEUP). It analyzes the parameter updates for the output layer and extracts information about the distribution of labels in the underlying training data of a model.

During the training process, the parameters of the output layer

neuron that represents the class of the currently considered sample are adapted slightly. Since this is repeated for every sample, neurons for frequent classes will be updated many times with high gradients⁴ such that the individual changes sum up to an update with a high magnitude for these neurons. On the other hand, if there are fewer (or no) samples of a class, there are fewer/no repetitions, resulting in an update with a low magnitude for such neurons. The total magnitudes of the updates for the neurons in the output layer leak therefore information about the frequency distribution of labels in the training data of this update.

For measuring the magnitudes and reverse engineer this distribution, we first define the Energy of the update for a neuron. Let H denote the number of connections of an output layer neuron to neurons of the previous layer, $b_{t,k,i}$ be the bias of neuron i from the output layer of a model k after round t , $w_{t,k,i,h}$ be analogously the weight of the connection to the neuron h from the previous layer, $b_{t,G_t,i}$ be as well as $w_{t,G_t,i,h}$ be analogously bias and weights of neurons from the global model G_t . Then the Energy $\mathcal{E}_{t,k,i}$ of the update for the output layer neuron i of the model that client k submitted in round t is given by:

$$\mathcal{E}_{t,k,i} = |b_{t,k,i} - b_{t,G_t,i}| + \sum_{h=0}^H |w_{t,k,i,h} - w_{t,G_t,i,h}| \quad (7)$$

If an Energy Update for a neuron is significantly higher than other Energy Updates for the same local model, then this indicates that the respective classes were more relevant for training the model. We normalize the Energy Updates of all output layer neurons of the same model, to highlight Energy Updates that are significantly higher than other Energy Updates. Therefore, the NormalizEd UPdate energy (NEUP) $\mathcal{C}_{t,k,i}$ of the neuron i for the update from client k in round t is given by:

$$\mathcal{C}_{t,k,i} = \frac{\mathcal{E}_{t,k,i}^2}{\sum_{j=0}^P \mathcal{E}_{t,k,j}^2} \quad (8)$$

The normalization makes the frequency distributions of different models comparable. Therefore, the individual NEUPs of a model update it not affected by the total extent of the Update Energy for this model update. Therefore, similar NEUPs from different models indicate that similar proportions of the training data of different clients have the same label. Moreover, it also makes the technique more robust against obfuscation by the adversary \mathcal{A} . Otherwise, \mathcal{A} could use one client to submit a model with a very high Energy Update to make the Energy Updates of the remaining poisoned models looking more similar to the benign ones.

In §VII, we provide a proof that the NEUPs are not affected, when \mathcal{A} scales the poisoned model updates.

C. Threshold Exceedings

The training data of poisoned models are significantly less heterogeneous than the training data of the benign models (cf. §III-E). For example, in the NLP scenario, the backdoor consists of a few sentences⁵, while the benign task includes

⁴When calculating the gradients of a NN for a sample x , the absolute magnitude of the gradients of the output layer neuron that represents the label of x is higher than the gradients for the other neurons [39].

⁵Otherwise the backdoor is significantly harder to inject (cf. App. A), allowing the other defense layers of DeepSight to mitigate the attack.

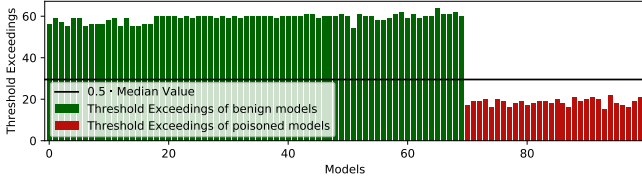


Fig. 3: NEUP Threshold Exceedings of benign and poisoned model updates

a large number of different sentences. We showed in §IV-B that the NEUPs allow a rough estimation of the distribution of labels in the training data of a client. Training data for poisoned models need to be focused on samples for the backdoor behavior (cf. §II-C). Therefore, if there is a local model with very homogeneous training data, then it is very likely that this model is poisoned. In the following, we introduce a metric entitled as *Threshold Exceedings* that measures the homogeneity of the training data and, by this is able to identify poisoned models. In §V-A, we will use the Threshold Exceedings to build a classifier for labeling all models as poisoned or benign. Our experiments confirmed a strong correlation between the NEUPs and the distribution of labels in the training data, s.t., the NEUPs can be used to measure the homogeneity of labels.

To measure the homogeneity of the NEUPs for the local models and therefore the complexity of the used training data, we define for each local model a threshold based on the maximal NEUP for this model. Then we count for each model how many NEUPs exceed this threshold.

If the output layer has P neurons, then the maximal NEUP $\mathcal{C}_{t,k,\max}$ of a model being submitted by client k in round t is given by:

$$\mathcal{C}_{t,k,\max} = \max_{1 \leq i \leq P} \mathcal{C}_{t,k,i} \quad (9)$$

We define the threshold $\xi_{t,k}$ as 1 % of the maximal NEUP $\mathcal{C}_{t,k,\max}$ of this client. However, as in scenarios with very few output labels, it is possible that all NEUPs of a client are above this threshold, we increase the Threshold Factor of 1 %, depending on the number of output classes. The threshold $\xi_{t,k}$ is, therefore, given by:

$$\xi_{t,k} = \max(0.01, 1/P) \cdot \mathcal{C}_{t,k,\max} \quad (10)$$

In App. I, we analyze the impact of different choices for the Threshold Factor on the Threshold Exceedings and DeepSight. The Threshold Exceedings value for a model is then given by the number of NEUPs that exceed this threshold. Let $\mathbb{1}_{expr}$ be the indicator function being 1 iff the expression *expr* is true and 0 otherwise, then the number of Threshold Exceedings $\text{TE}_{t,k}$ for a model being submitted by client k in round t is given by:

$$\text{TE}_{t,k} = \sum_{i=1}^P \mathbb{1}_{\mathcal{C}_{t,k,i} > \xi_{t,k}} \quad (11)$$

Figure 3 shows the NEUP Threshold Exceedings for the NIDS scenario for 70 benign and 30 poisoned model updates. As the figure shows, benign models have a significantly higher number of Threshold Exceedings than poisoned models.

For classifying model updates as benign or poisoned, we define a classification boundary of half of the median number of Threshold Exceedings. A model is labeled as poisoned, iff its number of Threshold Exceedings is below this threshold.

In §VII, we provide a proof that the Threshold Exceedings are not affected when \mathcal{A} scales the poisoned model updates.

V. MITIGATING BACKDOOR ATTACKS ON FL BY DEEP MODEL INSPECTION

Existing poisoning defenses often assume benign models to be similar, resulting in rejecting all abnormal model updates. However, those defenses can, due to the adopted approach, not distinguish between the reasons for perceiving a model as abnormal. Therefore, they cannot determine whether just different, non-IID data or poisoned data were used for training the model. As a result, those approaches will also reject models of benign clients with slightly deviating training data distributions. To solve this problem, we propose in the following DeepSight. It uses the proposed techniques to deeply inspect the model updates and distinguish between poisoned model updates and benign updates that have been trained on deviating data distributions. By using clipping [2], [28], [23], we enforce \mathcal{A} 's strategy to focus the training data of poisoned models on the backdoor behavior, s.t. the filtering scheme can effectively identify and exclude poisoned models. The basic structure of DeepSight is shown in Fig. 2. It consists of 3 layers:

1. Filtering Layer: The first layer uses the proposed novel techniques to analyze the model updates for detecting and excluding models that contain a well-trained backdoor.

2. Clipping Layer: This layer enforces a maximal L_2 -norm of the updates and downscales them if necessary to mitigate poisoned models that compensate a weakly trained backdoor (to circumvent the first layer) with a high scaling factor.

3. Aggregation Layer: The last layer uses FedAvg to aggregate the remaining, clipped updates together.

This combination of layers creates a dilemma for \mathcal{A} . If the poisoned models are suspicious, e.g., because they have been well-trained on homogeneous training data for achieving high backdoor impact, they will be detected and rejected by the filtering layer. Otherwise, if \mathcal{A} tries to circumvent the filtering layer by using heterogeneous training data, e.g., by using a low PDR or injecting complex backdoors, it also weakens the impact of the backdoor allowing the other two layers to mitigate the attack effectively.

A. Filtering Layer

The filtering layer recognizes poisoned models with homogeneous training data, by using a classifier that is based on the Threshold Exceedings (cf. §IV-C). To make the filtering more robust and minimize the number of mislabelings, we combine the classifier with a clustering to also take the labels of similar models into account when finally deciding about accepting or rejecting a model. To prevent

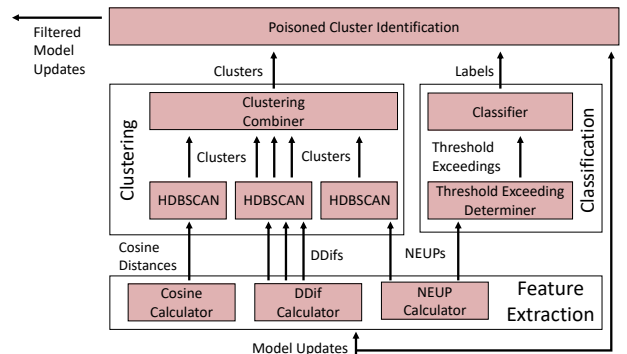


Fig. 4: Filtering Layer of DeepSight

Algorithm 1 Filtering Layer

```
1: Input: N, ▷ number of models
2: W, ▷ list of N received local models
3:  $G_t$  ▷ global model
4: Parameters:  $\tau$ , ▷ Threshold of suspicious models for excluding cluster
5: seeds, ▷ 3 seeds for generating random data for ddifs
6: input_dim ▷ dimension of a single input
7: Output: accepted_models
8: ▷ Feature Extraction
9: cosine_distances  $\leftarrow 0^{N \times N}$ 
10: global_bias  $\leftarrow$  output_layer_bias( $G_t$ )
11: for each clients  $i, j$  in  $[1, N]$  do
12:   update $_i$   $\leftarrow$  output_layer_bias( $W_i$ ) - global_bias
13:   update $_j$   $\leftarrow$  output_layer_bias( $W_j$ ) - global_bias
14:   cosine_distances $_{i,j}$   $\leftarrow 1 - \text{COSINE}(\text{update}_i, \text{update}_j)$ 
15: end for
16:  $\forall i \in \{1, \dots, N\}$  : neups $_i$   $\leftarrow$  NEUPs( $G_t, W_i$ )
17:  $\forall i \in \{1, \dots, N\}$  : thresh_exds $_i$   $\leftarrow$  THRESHOLD_EXCEEDING(neups)
18:  $\forall i \in \{1, 2, 3\}$  : rand_input_data $_i$   $\leftarrow$  random_matrix(seeds $_i$ , 20000, input_dim)
19:  $\forall i \in \{1, 2, 3\}$  : ddifs $_i$   $\leftarrow$  DDIFs(rand_input_data $_i, G_t, W_1 \dots W_n$ )
20: ▷ Classification
21: classificat_boundary  $\leftarrow$  MEDIAN(thresh_exds) / 2
22:  $\forall i \in \{1, \dots, N\}$  : labels $_i$   $\leftarrow$  (thresh_exds[i]  $\leq$  classificat_boundary)? 1:0
23: ▷ Clustering
24: clusters  $\leftarrow$  CLUSTER(N, neups, ddifs, cosine_distances)
25: ▷ PCI
26: accepted_models  $\leftarrow \{\}$ 
27: for cluster in clusters do
28:   amount_of_positives  $\leftarrow$  SUM(labels[cluster]) / |cluster|
29:   if amount_of_positives  $< \tau$  then
30:     accepted_models  $\leftarrow$  accepted_models  $\cup$  models[cluster]
31:   end if
32: end for
```

that \mathcal{A} can easily fool the similarity mechanism, we use an ensemble that is based on the NEUPs, DDifs, and cosine. \mathcal{A} would need to distract all of them at the same time, without reducing the attack impact, as otherwise the attack will be mitigated by the later defense layers.

The overall structure of the filtering layer is shown in Fig. 4. It first calculates features for the clustering (DDifs, NEUPs, and pairwise cosine distances) and uses these values in the next step for clustering all models. In parallel, the Threshold Exceedings are calculated from the NEUPs and used for labeling all model updates as benign or suspicious. In the last step, the Poisoned Cluster Identification (PCI) combines the clustering with the labeling to decide about accepting or rejecting the updates. The details are shown in Alg. 1. The algorithm takes as input the number of models, the local models, the global model, and the dimension of a single input.

1) *Feature Extraction:* First, we calculate the pairwise cosine distances, for each model $k \in \{1, \dots, N\}$, their corresponding NEUPs $\mathcal{C}_{t,k,*}$ and the Division Differences $\text{DDif}_{t,k,*}$ (cf. lines 8-19 in Alg. 1). As the DDifs depend on random input data, we calculate them three times with different input data that were generated by using different seeds.

An advantage of using the pairwise cosine distances of the updates, e.g., in comparison to using the Euclidean distances [4] is that its value does not change when \mathcal{A} scales its update (cf. App. H). The pairwise cosine of the updates is, therefore, more stable than other vector metrics.

2) *Classification:* To maximize the attack impact \mathcal{A} needs to use homogeneous training data (cf. §III-E). Otherwise, the attack will be mitigated by the later defense layers. The Threshold Exceedings measure the homogeneity of a model’s training data and uses it to label each model as benign or

Algorithm 2 Clustering

```
1: procedure DISTSFROMCLUST(clusters, N)
2:    $\forall i, j \in \{1, \dots, N\}$  : pairwise_dists $_{i,j}$   $\leftarrow$  cluster_of_model(i, clusters)
   == cluster_of_model(j, clusters)? 0:1 ▷ cluster_of_model(x, clusters)
   returns the cluster that contains the model with index x
3:   return pairwise_dists
4: end procedure
5:
6: Input:
7: N, ▷ N is the number of models
8: neups, ▷ NEUPs as list of N vectors with dimension P
9: ddifs ▷ DDifs as list of 3 lists of vectors with dimension P
10: cosine_distances ▷ cosine_distances a matrix  $\in \mathbb{R}^{N \times N}$ 
11: Output: clusters ▷ clusters as set of sets of indices
12:
13: cosine_clusters  $\leftarrow$  HDBSCAN(distances = cosine_distances)
14: cosine_cluster_dists  $\leftarrow$  DistsFromClust(cosine_clusters, N)
15: neup_clusters  $\leftarrow$  HDBSCAN(values = neups)
16: neup_cluster_dists  $\leftarrow$  DistsFromClust(NEUP_clusters, N)
17:  $\forall i \in \{1, 2, 3\}$  : ddif_clusters $_i$   $\leftarrow$  HDBSCAN(values = ddifs $_i$ )
18:  $\forall i \in \{1, 2, 3\}$  : ddif_clust_dists $_i$   $\leftarrow$  DistsFromClust(ddif_clusters $_i$ , N)
19: merged_ddif_clust_dists  $\leftarrow$  AVG(ddif_clust_dists $_1, \text{ddif\_clust\_dists}_2, \text{ddif\_clust\_dists}_3$ )
20: ▷ Combine clusterings
21: merged_distances  $\leftarrow$  AVG(merged_ddif_clust_dists, neup_clust_dists, cosine_clust_dists)
22: clusters  $\leftarrow$  HDBSCAN(distances = merged_distances)
```

suspicious, independently from other models (cf. lines 20-22 in Alg. 1).

The classifier calculates for each model $W_{t,k}$ the number of Threshold Exceedings (cf. §IV-C) and uses the median number of Threshold Exceedings divided by two as the classification boundary. A model is labeled as poisoned, if its number of Threshold Exceedings is below this threshold. As we assume the majority of clients to be benign (cf. §III-B), the median will always be at least as high as the lowest benign value.

3) *Clustering:* The goal of the clustering is to build groups of models, s.t. the training data of all models in the same group are based on IID training data and therefore all models should receive the same label. Because all clients use the same global model, clients with similar training data, will result in similar model updates (cf. §IV). Therefore, a clustering that is based on these features (DDifs, NEUPs and cosine distances), will create groups of models with similar training data. The clustering algorithm is shown in Alg. 2. In a scenario with P output classes of the models, the input for the algorithm is the number of models N , the NEUPs for each model as a list of N vectors with dimension P , the DDifs for 3 different seeds as a list of 3 lists, each containing N vectors of dimension P , as well as the pairwise cosine-distances for the updates of the output layer biases as a matrix of dimension $N \times N$.

The algorithm first clusters the cosine distances (cf. line 13 of Alg. 2), the NEUPs (cf. line 15 of Alg. 2) and the DDifs (cf. line 17 of Alg. 2). While the NEUPs and DDifs are clustered as plain values, the cosine distances are considered as a precomputed distance matrix. For the clustering HDBSCAN is used that determines the number of clusters dynamically. This allows DeepSight to build groups of models that optimally fit the data distributions and rather create more clusters than necessary than mixing models that were trained on data from different distributions, as this has the risk of mixing benign and poisoned models. A comparison of HDBSCAN with, e.g., k-means that is used Auror [34] is provided in App. B. This structure allows DeepSight to adapt the combination of techniques

dynamically to the current situation, addressing challenge C5. After clustering all feature values, a pairwise distance matrix is determined for each clustering by setting the distance between two models to 0 if they were put into the same cluster and otherwise 1 (cf. function `DistsFromClust` and lines 14, 16 and 18 in Alg. 2). First, the distance matrices for all DDif clusterings are combined via averaging (cf. line 19 in Alg. 2). Then, the result is averaged with the distance matrices for the cosines and NEUPs (cf. line 21 in Alg. 2). The resulting distance matrix is again processed by HDBSCAN as precomputed distance matrix (cf. line 25 in Alg. 2).

4) *Poisoned Cluster Identification (PCI)*: This component combines the results of the clustering and classification to finally decide about accepting or rejecting a model. To do so, it takes the clustering and labeling from the previous components and determines for each cluster the percentage of poisoned-labeled model updates (cf. lines 25 - 32 in Alg. 1). All models of a cluster remain if less than $\tau = 1/3$ of them are labeled as suspicious. Otherwise, all models of this cluster are removed. The component relies on the idea that all models in the same cluster have similar, IID training data and should, therefore, receive the same label. This mechanism in effect, therefore, realizes a voting about the label for all models in this cluster. The threshold of $\tau = 1/3$ was chosen as it is more likely that a poisoned model is labeled as benign than vice versa.

In summary, we build a dynamic filtering mechanism that efficiently identifies and filters poisoned models that were trained on homogeneous training data by deeply inspecting the predictions of the models and the parameters of the individual neurons. The filtering mechanism is not restricted to black-box metrics of model updates but deeply inspects the models, looking for artifacts of focused training data. It uses the Threshold Exceedings to label all models as suspicious or benign. It does not rely on a certain NN architecture nor backdoor types but inspects the models for artifacts that are characteristics for all backdoors and, therefore, addresses challenge C3. By analyzing the model updates for characteristics of poisoned models, it is able to effectively distinguish between poisoned and benign models, even if the benign models use deviating data. By this, DeepSight also addresses challenge C1.

The proposed techniques for inferring information about the training data of a model (DDifs, NEUPs) as well as the cosine metric build a stable clustering mechanism. It combines different kinds of features that make it, therefore, hard for an adversary to trick them. This clustering ensemble allows the filtering mechanism to create groups of models, where all data in the same group have IID training data. The clustering is used to support the classification and allow to consider their labels but also the labels of similar models for finally deciding about accepting or rejecting them. Moreover, by labeling each model separately, DeepSight is not forced to exclude models but is also free to accept all models. In addition, because of the high sensitivity of the PCI ($\tau = 1/3$), it is unlikely that models are accepted which are a threat for the aggregated model. On the other side, as we discussed in §IV-C, the Threshold Exceedings based identifier is unlikely to label benign clients as poisoned, addressing challenge C4. Therefore, the design realizes a well-balanced trade-off between being too restrictive and too open. We will discuss the effectiveness of the ensemble of different techniques further in §VI-C2.

B. Clipping Layer

To prevent \mathcal{A} from artificially increasing the weight of the poisoned model updates and, therefore, to ensure that \mathcal{A} focuses the training data on the backdoor behavior [28], we restrict the L_2 -norm of the individual updates to a boundary S by downscaling the updates if necessary, analogously to Eq. 3. The scaling factor for clipping a model $W_{t,i}$ that was trained by using the global model G_t is given by:

$$\lambda_{t,i}^c = \min \left(1, \frac{S}{\|W_{t,i} - G_t\|} \right) \quad (12)$$

Since the L_2 -norms of (benign) updates decrease during multiple rounds of training, it is challenging to determine a suitable static clipping boundary. Therefore, we choose S dynamically based on the median of the L_2 -norms of all updates, including the filtered model updates [28]. As we assume the majority of all clients to be benign, this value will always be in the interval of the L_2 -norms for the benign updates.

C. Aggregation Layer

In the aggregation layer, all remaining clipped models are aggregated together using FedAvg. However, in the last round, the aggregation is performed clusterwise and includes also the filtered, clipped models, s.t. only models from the same cluster are aggregated together and each client receives the model that was aggregated for the respective cluster.

As the clustering results in groups of models, where all models in the same group were trained on very similar, IID data this also separates models that were trained on benign or poisoned data. By applying this strategy we ensure that even if an adversary was able to circumvent the classifier in the first layer and even circumvent the clipping, the impact of the attack will be still restricted to the clients that \mathcal{A} already controls. This separation prevents the attack from affecting the benign clients. Moreover, if the global model of the previous round was already poisoned, this separation allows the benign clients to untrain the backdoor and gain a clean model, analogously to the concept of transfer learning [29].

VI. EVALUATION

A. Experimental Setup

To evaluate our approach, we test its effectiveness in three different FL applications. The first is the same NLP scenario that was already used by Bagdasaryan *et al.* [2] and allows a direct evaluation of DeepSight against their proposed attack, as it allows to replicate their experimental setup. Moreover, we also use the setup of Nguyen *et al.* [28] to allow a better comparison with existing defense approaches. In App. D, we evaluate DeepSight on multiple image datasets which are frequently used as benchmark datasets in FL [2], [38], [4], [28], [10], [37], [31].

1) *Text Prediction*: For the NLP scenario, we follow the experimental setup of Bagdasaryan *et al.* [2]. Therefore, we use the Reddit data set for November 2017. Each user with at least 150 and at most 500 posts was considered as one client. We created a dictionary and assigned an integer symbol to each of the most frequent 50000 words and included also three special symbols for unknown words as well as for the start and end of a post. The models used in this scenario consist of two LSTM layers with 200 hidden neurons each and a linear

TABLE I: Characteristics of used IoT datasets

Dataset	#devices	Time (hours)	Size (MiB)	Packets (millions)
<i>FLGuard-Benign</i>	18	4774.7	459.0	3528.3
<i>DIoT-Attack</i>	5	80.6	7734.2	21919.0
<i>DIoT-Benign</i>	10	1080.8	134.9	1062.9
<i>UNSW-Benign</i>	16	5415.6	2102.5	8564.4

output layer. After the model was trained for 5000 rounds with 100 randomly selected clients in each round, during which each client trained 2 epochs per round, the adversary used 10 malicious clients to inject advertisements and make the model, e.g., predict "delicious" after "pasta from astoria tastes". The Main Task Accuracy (MA) in this application refers to the accuracy of the suggested words.

2) *Network Intrusion Detection System (NIDS)*: Another application scenario is an FL-based NIDS for IoT devices [26]. We merged four different datasets containing traffic of IoT devices from real-world home and office deployments kindly made available to us by the authors of the respective papers [26], [28], [36]. Table I shows the details of the used datasets. The detection model consists of two layers with 128 Gated Recurrent Units (GRU) each and a linear output layer [26].

- 1) *FLGuard-Benign*: IoT traffic being captured in three real-world smart-home settings in different cities and one office for more than one week each [28].
- 2) *DIoT-Benign*: IoT traffic being captured in a real-world smart home with 18 IoT devices deployed [26].
- 3) *UNSW-Benign*: IoT traffic being captured in a small office with 28 IoT devices deployed [36].
- 4) *DIoT-Attack*: traffic of 5 IoT devices that were infected by the Mirai malware [26].

Following the setup of Nguyen *et al.* [28], we grouped the devices in the datasets according to their communication behavior, resulting in 44 distinct device type groups. We selected 22 device types that had sufficient data for distributing it over at least 15 simulated clients each having at least 2000 data samples. These device types represent different kinds of typical IoT devices found in a smart home, such as printers, smart light bulbs, smart plugs, or smart sensors. Depending on the amount of data available for a particular device type, its data were split into at least 15 and up to 200 clients, so that each client had between 2000 and 3000 samples for training. By doing this we ensure that the training data divided to different clients are as independent as possible and thereby resemble a real-world setting. Since different clients were assigned data from different data sets and different settings inside a dataset, the client data represent a combination of IID and non-IID data distributions. The detailed evaluation results of DeepSight for each of these device types can be found in App. C. For ease of presentation, we select the Netatmo Weather device, a smart weather station, as a representative example of a device type for the subsequent discussion, as it was present in three out of the four datasets and provided sufficient data to be distributed among 100 simulated clients.

Unless stated otherwise, we used for training the detection models a learning rate of 0.1 for benign clients, and for malicious clients the *constrain-and-scale* attack strategy with a learning rate of 0.01, a loss-control parameter $\alpha = 0.7$, a PDR of 50%, a PMR of 25%, and 10 local epochs. The initial global model was based on 10 rounds of be-

TABLE II: Effectiveness of DeepSight in comparison to existing defenses on NIDS and NLP dataset. The row *No defense* shows the impact of the *constrain-and-scale* attack with plain FedAvg.

Defenses	Text prediction				NIDS			
	BA	MA	PRC	NPV	BA	MA	PRC	NPV
<i>No Attack</i>	-	22.6	-	-	-	100.0	-	-
<i>No defense</i>	100.0	22.4	-	-	100.0	100.0	-	-
DP [2], [23]	21.9	20.6	-	-	14.8	82.3	-	-
Ensemble FL [6]	100.0	22.6	-	-	100.0	93.2	-	-
FoolsGold [10]	0.0	22.5	100.0	100.0	100.0	99.2	32.7	84.4
Auror [34]	100.0	22.4	-	90.0	100.0	96.6	0.0	70.2
AFA [24]	100.0	22.4	0.0	89.4	100.0	87.4	4.5	69.2
Krum [4]	100.0	22.6	9.1	0.0	100.0	84.0	24.2	0.0
FLGuard [28]	0.0	21.7	20.4	100.0	0.0	100.0	59.5	100.0
DeepSight	0.0	22.6	100.0	100.0	0.0	100.0	100.0	100.0

nign training before starting attacks. In the NIDS scenario, the Main Task Accuracy (MA) refers to the true negative rate, i.e., the rate of benign traffic being classified as benign whereas Backdoor Accuracy (BA) refers to the false-negative rate, i.e., the rate at which attack traffic samples of the adversary are erroneously classified as benign.

B. Experiment Platform

All experiments were performed on a server running Ubuntu 18.04 LTS, with 20 physical Intel Xeon CPU cores and 40 logical cores, 4 NVIDIA GeForce RTX 2080 Ti (each with 11GB memory), and 192 GB RAM. The experiments were implemented in Python, using the popular deep learning library Pytorch, the HDBSCAN implementation of McInnes *et al.* [20] and for evaluating existing work such as Auror [34] the machine learning library Scikit [30] was used.

C. Experimental Results

1) *Preventing Backdoor Attack*: Table II shows the effectiveness of DeepSight in comparison to several state-of-the-art defenses approaches in terms of BA, MA, precision (PRC), indicating the probability that a filtered model is indeed poisoned and its complement, the negative predictive value (NPV), indicating the probability that an accepted model is indeed benign. As can be seen, DeepSight effectively mitigates the attack in both scenarios. Other approaches [34], [4], [24] assume the data to be IID, which makes them fail for non-IID (Reddit) or partly IID (NIDS) data. Although FLGuard also achieves a decent performance in both scenarios, it also excludes many benign clients, which reduces the MA of the model, especially if it is applied from the beginning (cf. §VI-D). Also FoolsGold [10] achieves a decent performance in the text prediction scenario but fails for the IoT dataset. This is likely because FoolsGold assumes datasets of benign clients to be non-IID. The data in the IoT data set are partly IID (cf. §VI-A), causing FoolsGold to fail. On the other side, DeepSight is the only approach that is effective in both scenarios.

In App. F, we evaluate DeepSight against 5 different NLP and 12 NIDS backdoors, showing that it is not restricted to specific targets.

In most of our experiments, \mathcal{A} does not attack in the beginning but after several rounds of training, as otherwise there would be a high risk that, even if the attack would be successful, the later training would untrain the backdoor. To show, that this does not restrict \mathcal{A} , we conducted an experiment on the traffic of 5 different device types in the NIDS scenario, starting from a randomly initialized model and trained for 50 rounds. However, in all cases the BA remained at 0.

2) *Evaluation of Individual Components*: Table III compares the BA for the different layers of DeepSight, after running 10 rounds of training, while the malicious clients try to inject different numbers of phases from the Mirai botnet at the same time, using a PDR of 65 % and a learning rate of $10^{-2.5}$. We averaged the values over 9 very different device types, covering IoT devices for a wide spectrum of different applications with different behavior: Edimax Plug and TPLinkPlug (smart power plugs), DLinkType05 and EdnetGateway (collects of sensors, e.g., a door sensor), Lightify (a smart light bulb), NetatmoCam (a WIFI camera), PIX-STARPhoto-frame (a foto frame), Netatmo Weather and an HP Printer.

As the table shows, it is more difficult for \mathcal{A} to inject multiple backdoors at the same time, as already pointed out by Sun *et al.* [37]. It also shows that the clipping defense is not effective against simple backdoors, but is effective against complex backdoors since they have already a high L_2 -norm before they are scaled. On the other hand, filtering is effective in detecting backdoors that have a high imbalance in the underlying training data, but fails for complex backdoors. DeepSight combines the strengths of both and keeps the BA low for all backdoor complexities. This shows the effectiveness of the multi-layer strategy, where the filtering layer forces \mathcal{A} to weaken its attack when it wants to prevent the poisoned models from being filtered out. However, then the weakened attacks can be easily mitigated by the clipping layer of DeepSight.

In App. K, we analyze the effectiveness of the individual components of DeepSight’s filtering layer.

3) *Varying Attack Parameters*: For the *constrain-and-scale* attack strategy, \mathcal{A} can adjust different parameters of the training process for the malicious clients, with the purpose to overcome our defense. We evaluated different alpha-values from 0.1 to 1, different learning rates from 10^{-1} to 10^{-7} , different numbers of epochs from 1 to 100 and different stages of the training when \mathcal{A} starts its attack and runs the training process for each of them for at least 10 rounds for the NIDS dataset. Furthermore, we also evaluated different PMRs up to 45 % for 20 rounds to even evaluate the border cases. However, DeepSight was always able to classify the submitted models as benign or poisoned without any misclassifications. Therefore, the BA was always 0 % and the MA almost always 100 %.

We also evaluated different PDRs from 5 % to 100 %. Again, DeepSight did not misclassify any benign models. However, as already observed earlier for weakly-trained backdoors, which are realized here through low PDRs, DeepSight was not able to recognize all poisoned model updates. For a PDR of 5 %, DeepSight did not recognize any poisoned model updates and for PDRs of 8 % or 10 %, DeepSight failed to detect 6 out of 25 poisoned models. The reason for not recognizing some models for the PDRs of 8 % and 10 % is that the clustering put them together with benign models, but also the Threshold Exceedings based identifier did not recognize them correctly. For a PDR of 5 %, both, the clustering and the Threshold Exceedings based identifier failed. However, as we have demonstrated in §VI-C2, the clipping defense layer compensates the vulnerability of

TABLE III: BAs from DeepSight’s individual layers for different backdoor complexities, averaged over 9 IoT device types.

	1	2	3	4	13
No Defense	100.0 %	80.3 %	48.2 %	41.7 %	43.9 %
Clipping	87.5 %	56.2 %	31.2 %	13.9 %	11.5 %
Filtering	0.0 %	7.4 %	41.5 %	30.4 %	42.9 %
DeepSight	0.0 %	0.0 %	0.6 %	0.3 %	1.1 %

the filtering layer from DeepSight against such weak attacks. Because of the combination of both layers, the attack failed for all PDRs and the BA was always 0 %.

Therefore, the adversary can not circumvent DeepSight by varying the attack parameters.

4) *Sophisticated Attacks*: As we assume \mathcal{A} to have full knowledge about the system, it can adapt its strategy to circumvent DeepSight. In the following, we discuss three sophisticated attack strategies, specifically designed to overcome DeepSight and a recently proposed state-of-the-art backdoor attack [41]. In App. G, we evaluate another state-of-the-art attack [38] and two further adaptive attacks, targeting the clustering components of DeepSight by adding noise and use poisoned models to fill the gap between the benign and poisoned models.

Increasing Backdoor Complexity As the classifier labels models based on the complexity of their training data, a sophisticated adversary could try to increase the complexity for avoiding a focus on the backdoor target $C_{\mathcal{A}}$. We simulated this for the NIDS scenario by using the network traffic of multiple phases of the Mirai botnet. However, as shown in Tab. III, the BA is always close to zero. The reason for this is that for more complex backdoors the filtering component fails but on the other side, such backdoors are also harder to inject [37], causing them to be mitigated by the clipping layer. Also here the advantage of our multi-layer approach becomes visible.

Freeze Output Layer As the NEUPs and the Threshold Exceedings depend on the output layer updates, a sophisticated adversary could exclude the parameters of this layer from the training. To show the effectiveness of DeepSight, we run an experiment for the IoT-Traffic. We used different numbers of local epochs, up to 100 000 epochs and increased the PDR to 90 %. However, the BA of the local model did not increase, because it is significantly harder to train a model for a specific task without changing the output layer. Therefore, also the aggregated BA remains at 0 %, even for PMRs of more than 50 %, which goes beyond our attack scenario (cf. §III-B).

Adapt Anomaly Evasion Loss Another option is to consider the DDifs already during the training for the anomaly-evasion loss L_{anomaly} . We calculated the DDifs for the aggregation result of all benign models. L_{anomaly} was calculated as the L_2 -norm between the DDifs of this benign model and the current poisoned model. For simplicity, we used the actual benign models instead of estimations, as this strengthens \mathcal{A} , although this goes beyond our adversary model. However, even with this advantage, the attack was not successful. We run the experiment for 10 rounds, and different α values ($\alpha \in \{0.0, 0.1, \dots, 1.0\}$). Although the attack successfully distracted the DDifs, this was compensated by the other techniques. Therefore, DeepSight still completely mitigated the attack, showing the advantage of the clustering ensemble.

DBA Attack: Recently, Xie *et al.* introduced a novel backdoor attack strategy that split the trigger and the clients into different parts. Each group of clients only train for their respective trigger part [41]. We evaluated the attack in the NLP scenario. One group trained their models to predict the word ”delicious” 4 words after the word ”pasta”, the other group to predict ”delicious” 2 words after the word ”astoria”. However, although the attack achieved a BA of 64.5 % without defense, DeepSight successfully identified all poisoned models and mitigated the attack (BA=0 %), while keeping the MA at 22.6 %.

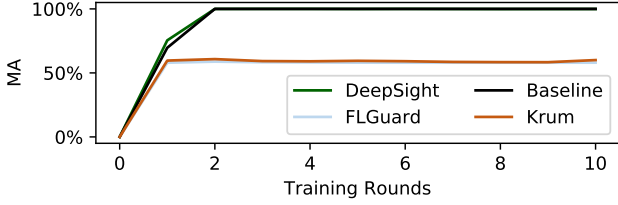


Fig. 5: Performance in terms of Main Task Accuracy (MA) of DeepSight and Krum [4] without attack

D. Impact on Benign Training Process

Several existing defense approaches [4], [24], work by excluding outliers and are, therefore, very likely to always exclude models even if there is no attack deployed. This impacts negatively the resulting model, causing a low MA and makes the respective defenses not practical.

Figure 5 compares the MA if no attack is deployed, for DeepSight, Krum [4], FLGuard [28] and without defense (Baseline), starting from a random model. As the figure shows, DeepSight slows down the training process slightly but achieves a good performance soon, similarly to the baseline. Therefore, the negative impact on the learning process is low. In comparison, Krum stops at 60%, as it always chooses a model representing data from the majority of clients. Analogously, also FLGuard does not consider outliers.

In App. J, we discuss the computational complexity of DeepSight. We show that the computationally expensive operations scale linearly with the number of participants, s.t., DeepSight causes only a low computational overhead.

We extensively evaluated various different attack strategies, including state-of-the-art attacks [2], [41], [38] as well as attacks that target the weak spots of DeepSight, e.g., adapting the anomaly-evasion loss function, freezing the output layer, reducing the attack impact or building clusters with a sufficient number of inconspicuous models. However, none of these attacks were effective in overcoming DeepSight. We showed that techniques that might be suitable for distracting DeepSight also reduce attack impact. Therefore, DeepSight addresses challenge C2. Moreover, also techniques like client-level Differential Privacy [23] do not have an impact on DeepSight, as we evaluated client-level model-noising with various different standard deviations and provide a proof for the robustness of the NEUPs, cosine distances and Threshold Exceedings against scaling/clipping the model updates (cf. §VII). Therefore, we showed that DeepSight effectively mitigates backdoor attacks.

VII. SECURITY CONSIDERATION

To achieve adversarial objective O1 (cf. §III-B), i.e., maximizing Backdoor Accuracy (BA), adversary \mathcal{A} needs to use a well-trained backdoor in its poisoned model updates to maximize its impact. Such model updates will, however, be identified and removed by model filtering. To avoid detection, \mathcal{A} can try to use only weakly trained backdoors. In this case, however, the attack is effectively mitigated by clipping. The filtering scheme is based on multiple measures (DDifs, NEUPs, Threshold Exceedings) to identify models with similar training data and label models as benign or malicious. Theorem 1 and Theorem 2 below show that neither DDifs nor Threshold Exceedings are affected if \mathcal{A} scales its model updates. Furthermore, also the cosine distances are shown to be resilient against scaling (cf. App.H).

Theorem 1. *The NEUPs are not affected by scaling or clipping the model update.*

Formally: Let G_t be the global model of an arbitrary round, $W_{t,k}$ an arbitrary local model applying update $U_{t,k}$, with $W_{t,k} = G_t + U_{t,k}$ and $NEUPs(G_t, W_{t,k})$ be the NEUPs for $W_{t,k}$.

$$\forall \lambda \in \mathbb{R} \setminus \{0\} : NEUPs(G_t, W_{t,k}) = NEUPs(G_t, G_t + \lambda U_{t,k})$$

Proof: See Appendix H. ■

Theorem 2. *The Threshold Exceedings are not affected by scaling or clipping the model update.*

Formally: Let G_t be the global model of an arbitrary round, $W_{t,k}$ an arbitrary local model applying update $U_{t,k}$, with $W_{t,k} = G_t + U_{t,k}$ and $TE(G_t, W_{t,k})$ be the Threshold Exceedings for $W_{t,k}$.

$$\forall \lambda \in \mathbb{R} \setminus \{0\} : TE(G_t, W_{t,k}) = TE(G_t, G_t + \lambda U_{t,k})$$

Proof: Follows immediately from Theorem 1, as the only input for the Threshold Exceedings are the NEUPs. ■

DeepSight relies on two values that are determined dynamically, the classification boundary for the Threshold Exceedings classifier and the clipping boundary. However, both values are calculated as the median of all values. As we assume the majority of clients to be benign, it is guaranteed that these values will always be in the range of benign values and, therefore, cannot be manipulated by \mathcal{A} .

Furthermore, we empirically showed that DeepSight effectively mitigates targeted poisoning attacks, including state-of-the-art attacks [2], [41], [38] as well as attacks targeting the weak spots of DeepSight against an arbitrarily behaving adversary. Therefore, DeepSight fulfills requirement R1 and prevents \mathcal{A} from achieving O1 and O2.

VIII. RELATED WORK

Various defenses against poisoning attacks in FL have been proposed. In the following, we will discuss and compare them to DeepSight.

A. Anomaly Detection-Based Approaches

Many backdoor defenses follow an outlier-detection-based strategy and exclude anomalous model updates [34], [4], [24], [42], [15], [14], [16], [12]. They assume that the local data of all benign clients are similar, i.e., identically and independently distributed (IID), so that it is sufficient to filter models that differ from the majority of models. However, in many scenarios the data are non-IID [10], [35], resulting in differences among benign models. Therefore, many benign models are excluded, causing the resulting model to perform worse on the data of the excluded local models (cf. §VI-D).

Krum aggregates local models by choosing a single local model as the aggregated model with the smallest Euclidean distance to a certain fraction of other models [4]. Hence, models trained on deviating data will never be chosen.

Munoz *et al.* exclude a local model if its cosine distance to the aggregated model is higher or lower than the median distance plus/minus the standard deviation [24]. Unfortunately, also this approach suffers from a high false-positive rate (cf. §VI-C1).

Baffle sends the aggregated model to a randomly selected subset of clients. Those so-called validation clients evaluate

the model on their local data and vote about accepting the aggregated model or rejecting it [1]. However, validation clients can only notice the backdoor if they have a sufficient number of trigger samples or the backdoor attack has a significant impact on the model’s behavior on the main task. The first scenario is not realistic, as benign clients can not be assumed to have knowledge of trigger samples. The second scenario implies that the attack is not stealthy, violating O2 (cf. §III-B), and making the backdoor easy to detect. Furthermore, the approach does not work if the data of a (small) number of training clients differs from the majority of validation clients, which happens, e.g., in non-IID scenarios. Also, Baffle cannot be used from the beginning but, e.g., only after several hundreds of rounds, as otherwise many false positives will occur (cf. [1]).

Auror first determines indicative features by clustering for each parameter all local models separately using k-means with two clusters. It selects features with the highest distances between the two centroids. A model is rejected if it was clustered for too many indicative features to the smaller cluster [34]. Also Auror focuses on excluding outliers. Moreover, a centroid-based clustering can be successfully distracted (cf. App B). FLGuard also exploits the dilemma of \mathcal{A} to either focus on the training data and getting filtered, or to use weakly-trained model updates, allowing the clipping layer to mitigate the attack. Nguyen *et al.* combine an outlier-based clustering with clipping and adding random noise to the model [28]. However, while DeepSight uses a classifier for identifying poisoned model updates, FLGuard uses a clustering approach that rejects outliers, including benign model updates that were trained on different data (cf. §VI-D).

Liu *et al.* introduced another approach to detect backdoored models in centralized settings [17]. However, their approach is not suitable for FL settings and does not consider semantic backdoor attacks as discussed in detail in App. L.

In summary, besides being ineffective (cf. §VI-C1), existing filtering approaches for FL also neglect a main principle of FL by preventing utilizing the data of different clients, as the resulting model was trained only on data of a certain group of clients (cf. § VI-D).

B. Other Defense approaches

FoolsGold [10] assumes that benign datasets from different clients differ from each other and assigns low weights to models, which are similar to many other models. However, this harms the impact of benign clients with similar data. For example, in the case of the NIDS scenario, the network traffic does not vary much because of the limited functionalities of an IoT device. Moreover, FoolsGold sums up the updates for all rounds and compares them, instead of focusing on the current round. This allows a sophisticated adversary to submit poisoned updates without being perceived as suspicious.

Differential Privacy [23] enforces a maximal, static L_2 -norm of the updates and adds randomly generated noise. As pointed out by Bagdasaryan *et al.* it has the side effect of also mitigating backdoor attacks [2]. However, it fails for well-trained poisoned models (cf. §VI).

Other approaches [42], [12] calculate the median for all parameters and, therefore, also focus on models, representing the majority but neglect models that were trained on different training data. Moreover, also these defenses have shown to be vulnerable to different poisoning attacks [8].

The approach of Cao *et al.* trains multiple models. For

each of these models, a random subset of clients is used for training a model over multiple rounds. At inference time, each resulting global model is applied and the final prediction is determined via majority voting. Cao *et al.* prove that if the training is completed, they could determine for a specific sample a minimal number m of malicious clients, which their algorithm would have been able to tolerate [6]. Unfortunately, this number can differ arbitrarily for different input samples. Moreover, their proof does not provide any work in practice. Since determining this number requires a-posteriori knowledge, the impact of determining m at this point is negligible, as the models are already trained and it is, therefore, too late to prevent backdoor attacks. Furthermore, at this point, it is not even clear, whether the current label for the considered samples is even correct or a backdoor attack already took place and flipped the label already. Finally, the approach is vulnerable for the replacement-scaling attack of Bagdasaryan *et al.* [2] and damages the MA, as we demonstrated in §VI-C1, and fails even for low PMRs of 5 % (cf. [6]).

C. Model Inference Attacks in FL

Different approaches to inference information from models have been proposed [39], [13], [25], [32]. Although these approaches work well to violate the users’ privacy in the considered attack scenarios, none of them is suitable for being used on an FL aggregation server to identify poisoned model updates. Membership inference attacks that determine the presence of a specific sample [13], [25], are not effective as benign and poisoned samples can overlap, e.g., for the NIDS scenario. Other approaches, require attackers to have their own training data [32], which is not practical for the FL server (cf. §III-C), or train separate models for each label [39], making the approach not practical, e.g., for the NLP scenario with 50 000 words.

In comparison, the techniques that were proposed in this paper (NEUPs, DDifs, and Threshold Exceedings), allow to estimate information about the training data distribution and identify poisoned models and models with similar data but causes only a small computational overhead (cf. App. J) and do not require test data to be available on the aggregation server.

IX. CONCLUSION

Backdoor attacks threaten the integrity of Federated Learning (FL), which is a promising emerging technology. We show that existing countermeasures cannot adequately address sophisticated backdoor attacks on FL and introduce DeepSight, a novel model filtering approach that effectively mitigates backdoor attacks on FL. While existing backdoor defenses are often restricted to excluding abnormal models, DeepSight follows an orthogonal approach by using several novel techniques to conduct a deep inspection of the submitted models separately for identifying and excluding poisoned models.

We present several new techniques (DDifs, NEUPs, Threshold Exceedings) to infer information about a model’s training data, identify similar models, and measure the homogeneity of model updates. By performing a deep inspection of the models’ structure and their predictions, DeepSight can effectively mitigate state-of-the-art poisoning attacks and is robust against sophisticated attacks, without degrading the performance of the aggregated model.

Recently, different secure aggregation schemes have been

proposed preventing the aggregation server from accessing the individual model updates [5], [9]. Although, DeepSight does not reduce the privacy level compared to FedAvg [21] as it also anonymizes the individual contributions and smoothens the parameter updates by aggregating them, future work needs to implement a privacy-preserving version of DeepSight to combine the privacy gains of secure aggregations with the backdoor mitigation algorithm of DeepSight.

ACKNOWLEDGMENT

We thank the anonymous reviewers and the shepherd for constructive reviews and comments. We further want to thank Intel Private AI center and BMBF and HMWK within ATHENE project for their support of this research.

REFERENCES

- [1] S. Andreina, G. A. Marson, H. Möllering, and G. Karame, “BaF-FL: Backdoor Detection via Feedback-based Federated Learning,” in *ICDCS*, 2021.
- [2] E. Bagdasaryan, A. Veit, Y. Hua, D. Estrin, and V. Shmatikov, “How to backdoor federated learning,” in *International Conference on Artificial Intelligence and Statistics (AISTATS)*. PMLR, 2020.
- [3] M. Baruch, G. Baruch, and Y. Goldberg, “A Little Is Enough: Circumventing Defenses For Distributed Learning,” in *Advances in Neural Information Processing Systems (NIPS)*, 2019.
- [4] P. Blanchard, E. M. El Mhamdi, R. Guerraoui, and J. Stainer, “Machine Learning with Adversaries: Byzantine Tolerant Gradient Descent,” in *Advances in Neural Information Processing Systems (NIPS)*, 2017.
- [5] K. Bonawitz, V. Ivanov, B. Kreuter, A. Marcedone, B. McMahan, S. Patel, D. Ramage, A. Segal, and K. Seth, “Practical Secure Aggregation for Privacy-Preserving Machine Learning,” in *CCS*, 2017.
- [6] X. Cao, J. Jia, and N. Z. Gong, “Provably secure federated learning against malicious clients,” *AAAI Conference on Artificial Intelligence*, 2021.
- [7] S. Chopra, R. Hadsell, and Y. LeCun, “Learning a similarity metric discriminatively, with application to face verification,” in *Computer Society Conference on Computer Vision and Pattern Recognition (CVPR)*. IEEE, 2005.
- [8] M. Fang, X. Cao, J. Jia, and N. Zhenqiang Gong, “Local Model Poisoning Attacks to Byzantine-Robust Federated Learning,” in *USENIX Security*, 2020.
- [9] H. Fereidooni, S. Marchal, M. Miettinen, A. Mirhoseini, H. Möllering, T. D. Nguyen, P. Rieger, A.-R. Sadeghi, T. Schneider, H. Yalame, and S. Zeitouni, “SAFElearn: secure aggregation for private federated learning,” in *IEEE Security and Privacy Workshops (SPW)*. IEEE, 2021.
- [10] C. Fung, C. J. Yoon, and I. Beschastnikh, “The limitations of federated learning in sybil settings,” in *International Symposium on Research in Attacks, Intrusions and Defenses (RAID)*, 2020.
- [11] GoogleLLC, “Gboard - the google keyboard,” <https://play.google.com/store/apps/details?id=com.google.android.inputmethod.latin>.
- [12] R. Guerraoui, S. Rouault *et al.*, “The hidden vulnerability of distributed learning in byzantium,” in *International Conference on Machine Learning (ICML)*, 2018.
- [13] J. Hayes, L. Melis, G. Danezis, and E. De Cristofaro, “Logan: Membership inference attacks against generative models,” in *Privacy Enhancing Technologies*, 2019.
- [14] Y. Khazbak, T. Tan, and G. Cao, “Mlguard: Mitigating poisoning attacks in privacy preserving distributed collaborative learning,” in *International Conference on Computer Communications and Networks (ICCCN)*. IEEE, 2020.
- [15] S. Li, Y. Cheng, Y. Liu, W. Wang, and T. Chen, “Abnormal client behavior detection in federated learning,” *arXiv preprint arXiv:1910.09933*, 2019.
- [16] S. Li, Y. Cheng, W. Wang, Y. Liu, and T. Chen, “Learning to detect malicious clients for robust federated learning,” *arXiv preprint arXiv:2002.00211*, 2020.
- [17] Y. Liu, W.-C. Lee, G. Tao, S. Ma, Y. Aafer, and X. Zhang, “Abs: Scanning neural networks for back-doors by artificial brain stimulation,” in *ACM SIGSAC Conference on Computer and Communications Security*, 2019.
- [18] Y. Liu, S. Ma, Y. Aafer, W.-C. Lee, J. Zhai, W. Wang, and X. Zhang, “Trojaning attack on neural networks,” in *NDSS*, 2018.
- [19] S. Lloyd, “Least squares quantization in pcm,” *IEEE transactions on information theory*, vol. 28, no. 2, 1982.
- [20] L. McInnes, J. Healy, and S. Astels, “hdbscan: Hierarchical density based clustering,” *The Journal of Open Source Software*, 2017.
- [21] B. McMahan, E. Moore, D. Ramage, S. Hampson, and B. A. y Arcas, “Communication-Efficient Learning of Deep Networks from Decentralized Data,” in *International Conference on Artificial Intelligence and Statistics (AISTATS)*, 2017.
- [22] B. McMahan and D. Ramage, “Federated learning: Collaborative Machine Learning without Centralized Training Data,” in *Google Research Blog*. Google AI, 2017, <https://ai.googleblog.com/2017/04/federated-learning-collaborative.html>.
- [23] B. McMahan, D. Ramage, K. Talwar, and L. Zhang, “Learning differentially private recurrent language models,” in *International Conference on Learning Representations (ICLR)*, 2018.
- [24] L. Muñoz-González, K. T. Co, and E. C. Lupu, “Byzantine-Robust Federated Machine Learning through Adaptive Model Averaging,” in *arXiv preprint:1909.05125*, 2019.
- [25] M. Nasr, R. Shokri, and A. Houmansadr, “Comprehensive privacy analysis of deep learning: Passive and active white-box inference attacks against centralized and federated learning,” in *S&P*. IEEE, 2019.
- [26] T. D. Nguyen, S. Marchal, M. Miettinen, H. Fereidooni, N. Asokan, and A. Sadeghi, “DfIoT: A Federated Self-learning Anomaly Detection System for IoT,” in *ICDCS*, 2019.
- [27] T. D. Nguyen, P. Rieger, M. Miettinen, and A.-R. Sadeghi, “Poisoning Attacks on Federated Learning-Based IoT Intrusion Detection System,” in *Workshop on Decentralized IoT Systems and Security (DISS) @ NDSS*, 2020.
- [28] T. D. Nguyen, P. Rieger, H. Yalame, H. Möllering, H. Fereidooni, S. Marchal, M. Miettinen, A. Mirhoseini, A.-R. Sadeghi, T. Schneider *et al.*, “FLGUARD: Secure and Private Federated Learning,” *arXiv preprint arXiv:2101.02281*, 2021.
- [29] S. J. Pan and Q. Yang, “A survey on transfer learning,” *IEEE Transactions on knowledge and data engineering*, vol. 22, no. 10, 2009.
- [30] F. Pedregosa, G. Varoquaux, A. Gramfort, V. Michel, B. Thirion, O. Grisel, M. Blondel, P. Prettenhofer, R. Weiss, V. Dubourg, J. Vanderplas, A. Passos, D. Cournapeau, M. Brucher, M. Perrot, and E. Duchesnay, “Scikit-learn: Machine Learning in Python,” *Journal of Machine Learning Research*, 2011.
- [31] L. Rieger, R. M. T. Høegh, and L. K. Hansen, “Client adaptation improves federated learning with simulated non-iid clients,” in *International Workshop on Federated Learning for User Privacy and Data Confidentiality in Conjunction with ICML 2020*. International Machine Learning Society (IMLS), 2020.
- [32] A. Salem, A. Bhattacharya, M. Backes, M. Fritz, and Y. Zhang, “Updates-leak: Data set inference and reconstruction attacks in online learning,” in *USENIX Security*, 2020.
- [33] M. Sheller, A. Reina, B. Edwards, J. Martín, and S. Bakas, “Federated Learning for Medical Imaging,” in *Intel AI*, 2018, <https://www.intel.com/content/www/us/en/artificial-intelligence/posts/federated-learning-for-medical-imaging.html>.
- [34] S. Shen, S. Tople, and P. Saxena, “Auror: Defending Against Poisoning Attacks in Collaborative Deep Learning Systems,” in *Annual Computer Security Applications Conference (ACSAC)*, 2016.
- [35] R. Shokri and V. Shmatikov, “Privacy-Preserving Deep Learning,” in *CCS*, 2015.
- [36] A. Sivanathan, H. H. Gharakheili, F. Loi, A. Radford, C. Wijenayake, A. Vishwanath, and V. Sivaraman, “Classifying IoT Devices in Smart Environments Using Network Traffic Characteristics,” in *IEEE Transactions on Mobile Computing*, 2018.
- [37] Z. Sun, P. Kairouz, A. T. Suresh, and H. B. McMahan, “Can you really backdoor federated learning?” *arXiv preprint arXiv:1911.07963*, 2019.

- [38] H. Wang, K. Sreenivasan, S. Rajput, H. Vishwakarma, S. Agarwal, J.-y. Sohn, K. Lee, and D. Papailiopoulos, "Attack of the tails: Yes, you really can backdoor federated learning," in *NeurIPS*, 2020.
- [39] L. Wang, S. Xu, X. Wang, and Q. Zhu, "Eavesdrop the Composition Proportion of Training Labels in Federated Learning," *arXiv preprint:1910.06044*, 2019.
- [40] S. Wold, K. Esbensen, and P. Geladi, "Principal component analysis," in *Chemometrics and intelligent laboratory systems*, vol. 2. Elsevier, 1987.
- [41] C. Xie, K. Huang, P.-Y. Chen, and B. Li, "Dba: Distributed backdoor attacks against federated learning," in *International Conference on Learning Representations (ICLR)*, 2019.
- [42] D. Yin, Y. Chen, R. Kannan, and P. Bartlett, "Byzantine-robust distributed learning: Towards optimal statistical rates," in *International Conference on Machine Learning (ICML)*, 2018.

APPENDIX

A. Homogeneity of Poisoned Models

Although the adversary \mathcal{A} needs to craft inconspicuous models for preventing a detection or mitigation of its attack (O2; cf. §III-B), this also reduces the attack impact (O1). In the following, we will show that, in order to run a successful attack, \mathcal{A} needs to focus on the backdoor behavior, resulting in homogeneous model updates. To make the models more inconspicuous, \mathcal{A} can tune the PDR and also make the backdoor behavior more complex for imitating a deviating distribution of benign training data.

Backdoor Complexity As pointed out by Sun *et al.* [37] and also confirmed by our experiments (cf. §VI-C2), increasing the complexity of the backdoor behavior also significantly reduces the attack impact. If, i.e., \mathcal{A} includes 4 phases of Mirai in its backdoor for the NIDS scenario, this reduces the attack impact even without defense and allows a defense that only consists of the clipping component (cf. §V-B) to reduce the BA to 13.9%, indicating that \mathcal{A} cannot increase backdoor complexity beyond this value. On the other side, the filtering is still effective, showing that even for this complexity level, the training data are homogeneous enough to get detected by DeepSight.

PDR: The second parameter that affects the homogeneity of models is the PDR. However, as pointed out by Nguyen *et al.*, low PDRs also reduce the attack impact and increase the risk that the impact of the poisoned model updates becomes

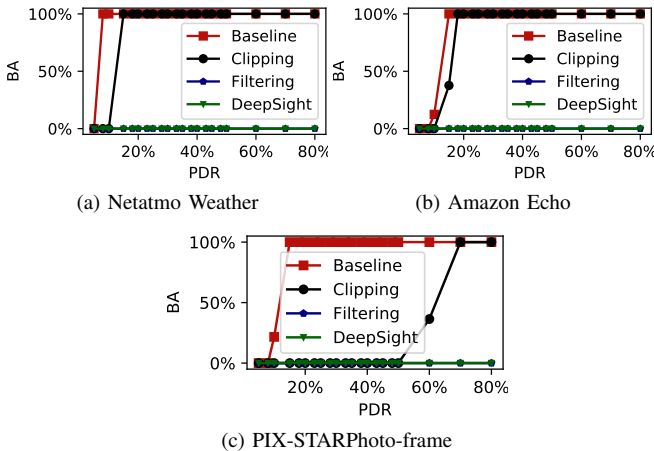


Fig. 6: Impact of the Poisoned Data Rate (PDR) on the Backdoor Accuracy (BA) without defense, a clipping defense (§V-B), filtering (§V-A) and DeepSight for different device types.

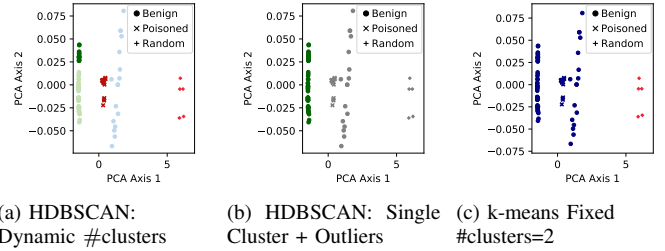


Fig. 7: Effectiveness of our clustering algorithm (a) compared to HDBSCAN for a single cluster and outliers (grey) [28] (b) as well as k-means clustering [34] (c). The individual models are visualized by using the principal component analysis (PCA⁶).

negligible during the aggregation. Figure 6 shows the BA for the individual components for three different device types, depending on the PDR. Also here, clipping mitigates the attack successfully for low PDRs but fails for high values. Therefore, to achieve a high attack impact, especially in scenarios where the server applies clipping, \mathcal{A} needs to use a high PDR, i.e. at least 20%. However, this causes a focus of the poisoned training data on the attack data, resulting in homogeneous model updates, which allows the filtering layer to detect and filter the poisoned models.

In summary, if \mathcal{A} tries to increase the heterogeneity of its model updates by, e.g., reducing the PDR or making the backdoor behavior more complex, the impact of the backdoor will simultaneously also decrease the attack impact, making it easier to be mitigated by defenses like weight clipping (cf. §V-B). Therefore, to maximize the attack impact, \mathcal{A} needs to choose a high PDR and a simple backdoor behavior, causing the training data to differ from the benign data and causing the model updates to be more homogeneous, thus making them distinguishable from benign ones.

B. Comparison of Clustering Approaches

DeepSight uses HDBSCAN for clustering. Other clustering algorithms, e.g., k-means [19] that is used by Auror [34] have, among others, the disadvantage to require the number of clusters in advance. However, this can be exploited by \mathcal{A} to circumvent the defense, as shown in Fig. 7. This figure compares HDBSCAN against k-means for the NIDS dataset with 25 malicious clients. To distract the defense, \mathcal{A} used a subset of 5 clients for submitting random model updates. As subfigure 7c shows, this successfully distracts k-means, s.t. it accepts the remaining poisoned models, while HDBSCAN is not distracted by the random models. However, the version that accepts only a single cluster also rejects many benign models. On the other side, the plain HDBSCAN is well suited for distinguishing model updates, trained on different data. It effectively separates all different groups of models.

C. Performance of DeepSight on the IoT dataset

Table IV shows the performance of DeepSight for all device types in the NIDS scenario. As the table shows, DeepSight successfully mitigates all backdoor attacks, although it does not always filter all poisoned models. For example, in case of the Ednet Gateway, the filtering does not filter any malicious client,

⁶The Principal Component Analysis (PCA) is a well-known technique to extract principal dimensions from high-dimensional data [40].

TABLE IV: Main Task Accuracy (MA), Backdoor accuracy (BA), Poisoned Probability (PRC) and Benign Probability (NPV) of DeepSight for different IoT devices in the NIDS scenario.

Device Type	No Defense		DeepSight			
	BA	MA	BA	MA	PRC	NPV
Amazon Echo	100.0	99.9	0.0	93.3	100.0	100.0
Belkin Wemo Motion Sensor	100.0	99.9	0.0	99.2	92.6	100.0
DLink Type05	100.0	91.9	0.0	98.3	100.0	98.7
Edimax Plug	100.0	98.7	0.0	98.8	100.0	100.0
Ednet Gateway	100.0	100.0	0.0	100.0	-	75.0
Google Home	58.2	100.0	0.0	87.5	100.0	100.0
HP Printer	100.0	92.6	0.0	89.9	100.0	100.0
Insteon Camera	100.0	98.9	0.0	97.8	100.0	98.7
LiFx Light Bulb	100.0	100.0	0.0	83.7	100.0	90.5
Lightify2	100.0	100.0	0.0	100.0	100.0	100.0
Nest Dropcam	100.0	100.0	0.0	100.0	100.0	84.6
Netatmo Cam	100.0	100.0	0.0	100.0	100.0	100.0
Netatmo Weather	0.0	93.5	0.0	100.0	100.0	100.0
PIX-STARPhoto-frame	100.0	100.0	0.0	99.9	100.0	100.0
Samsung Smart Cam	100.0	99.2	0.0	99.9	100.0	100.0
Smarter	100.0	100.0	0.0	100.0	100.0	100.0
TP-Link Cloud Camera	100.0	98.6	0.0	97.6	100.0	100.0
TPLink Plug	0.0	89.1	0.0	100.0	100.0	83.3
Tesvor Vacuum	100.0	96.1	0.0	95.5	100.0	100.0
Triby Speaker	0.0	81.5	0.0	80.8	100.0	100.0
Wemo Switch	100.0	100.0	0.0	100.0	100.0	100.0
Withings Sleep Sensor	100.0	100.0	0.0	100.0	100.0	100.0
Withings Baby Monitor	100.0	100.0	0.0	100.0	100.0	100.0
iHome	100.0	92.2	0.0	92.9	100.0	100.0
Average	85.8	97.2	0.0	96.5	99.7	97.1

since the Threshold Exceedings of most poisoned models (on average 27.75) are slightly higher than the boundary (29, the benign models have in average 57 Threshold Exceedings). However, as the clipping boundary is always in the interval of benign values and the benign and poisoned models are separated, the BA is still 0%, showing the effectiveness of our multi-layer approach.

D. Evaluation of DeepSight on Image Datasets

The CIFAR-10 and MNIST datasets are frequently used as benchmark datasets for FL. [2], [38], [4], [28], [10], [37], [31]. To allow a better comparison with other work on FL, we replicate the setup of existing work. For the CIFAR-10 dataset, we use a light version of Resnet-18 model and an IID rate of 0.7. The adversary aims to make cars in front of a stripped background being classified as birds [2], [28]. For MNIST, the model consists of 2 convolutional layers with a max-pooling in between and 2 fully connected layers [6]. The adversary aims to make pictures with a white rectangle on the left side to be classified as a "0". We used 100 clients and set the PMR to 20 % [28]. As Tab. V shows, DeepSight effectively mitigates the attack, while without defense the BA reaches 100% and 96.3%. It is worth noting, that in case of MNIST sometimes misclassifications are counted in favor of the BA (cf. §G).

In App. E, we evaluate DeepSight for an image recognition scenario, where the dataset of each client consists only of a single label to simulate homogeneous benign training data.

E. Scenarios with a Single Source Label

The Threshold Exceedings classifier of DeepSight estimates the homogeneity of the used training data based on the distribution of labels. However, in special scenarios the local datasets of each client might consist only of samples with a single label, e.g., for facial user authentication on smartphones. Although, in those scenarios a binary classifier or a siamese network [7] might be more suitable than FL, we performed an additional experiment on the popular CIFAR-10 benchmark

TABLE V: Effectiveness of DeepSight for the CIFAR-10 and MNIST datasets. All values in percentage

Defense	CIFAR-10				MNIST			
	BA	MA	PRC	NPV	BA	MA	PRC	NPV
No Attack	0.0	92.2	-	-	0.4	95.7	-	-
No Defense	100.0	84.1	-	-	96.3	58.9	-	-
DeepSight	0.0	92.2	-	80	0.3	96.6	100	100

dataset with 100 clients and a PMR of 20 % to demonstrate DeepSight’s effectiveness even in those scenarios. As Tab. VIII shows, although DeepSight did not detect the malicious models, the later defense layers successfully mitigated the attack. Table VIII also shows that due to the dynamic threshold of the Threshold Exceedings classifier, DeepSight did not raise any false positive, demonstrating that DeepSight does not negatively affect the MA of the resulting model.

F. Performance of DeepSight against Different Backdoors

To demonstrate that DeepSight is not restricted to certain attack patterns, we evaluate it against different backdoors.

NIDS: We evaluated DeepSight against different backdoors in the NIDS scenario, by using different attack modes of the Mirai malware as attack traffic. As Tab. VI shows, DeepSight effectively mitigates all of these attacks.

Word Prediction: We injected different sentences, which were also used by Bagdasaryan *et al.* [2]. As Tab. VII shows, DeepSight is effective against all of these backdoors.

G. Further Sophisticated Backdoor Attacks

Edge Case: Wang *et al.* recently proposed an attack that aims to flip the labels for the samples, where the adversary’s focus on samples where the predictions are already made with a low confidence value. Therefore, the attack targets samples where the predicted probability is low, although it is still classified correctly [38]. We followed their experimental setup of and conducted an experiment for the CIFAR-10 benchmark dataset for 1500 rounds. In each round 10 clients were randomly selected for training their local model. The adversary \mathcal{A} launched its attack for 150 rounds. Without defense, \mathcal{A} achieved a BA of 53.06% and a MA of 86.46 %. DeepSight reduced the BA to 7.14 % and the MA to 80.54 % and, therefore, successfully mitigated the attack. It is worth noting that even without attack the BA is 11.2% and the MA is 77.53% as here also misclassifications are considered.

Model Noising DeepSight uses clustering in several places to identify clients with similar training data. Therefore, a sophisticated adversary could add random noise to the poisoned

TABLE VI: Main Task Accuracy (MA), Backdoor accuracy (BA), Poisoned Probability (PRC) and Benign Probability (NPV) of DeepSight for different NIDS backdoors.

Backdoor	No Defense		DeepSight			
	BA	MA	BA	MA	PRC	NPV
Dos-ACK	100.0	92.8	0.0	100.0	100.0	100.0
Dos-DNS	100.0	98.0	0.0	100.0	100.0	100.0
Dos-Greeth	100.0	98.1	0.0	100.0	100.0	100.0
Dos-Greip	100.0	97.5	0.0	100.0	100.0	100.0
Dos-HTTP	100.0	92.5	0.0	100.0	100.0	100.0
Dos-Stomp	100.0	97.5	0.0	100.0	100.0	100.0
Dos-SYN	100.0	82.0	0.0	100.0	100.0	100.0
Dos-UDP	100.0	92.9	0.0	100.0	100.0	100.0
Dos-UDP (Plain)	100.0	96.5	0.0	100.0	100.0	100.0
Dos-VSE	100.0	97.2	0.0	100.0	100.0	100.0
Preinfection	100.0	98.0	0.0	100.0	100.0	100.0
Scanning	100.0	82.0	0.0	100.0	100.0	100.0
Average	100.0	93.7	0.0	100.0	100.0	100.0

models, in order to distract DeepSight. We evaluated this attack by adding noise with 36 different standard deviations from $4.3 \cdot 10^{-17}$ to 21.5 (logarithmically distributed) with a mean of 0 for the NIDS scenario. However, this attack failed, as the BA was always 0 even for the highest standard deviations, which was too high, indicated by low BA values for the noised poisoned local models.

Gap Bridging As DeepSight uses a voting-based filtering mechanism to evaluate the models of a cluster, a sophisticated adversary could try to use a few of the poisoned models, to connect the benign cluster with the cluster that contains all poisoned models, such that they are merged and the benign models cause the cluster to be accepted. We used 200 clients with a PMR of 40% and split all malicious clients into different groups, with a gradually increasing PDR from 5% to 20%. However, although 19 models with a very low PDR were accepted, the majority of poisoned models were rejected but not a single benign model. The BA was 0% and the MA 100%. This also shows the advantage of the ensemble, as a naive clustering approach, using only the cosines and k-means, fails and does not filter any poisoned model, while DeepSight identifies most of the poisoned models and successfully mitigates the impact of the no recognized models.

H. Stability of Metrics against scaling

The adversary can scale the updates, either to increase the impact or as part of techniques like client-level DP, to make them less suspicious. In the following, we show that the cosine and NEUPs are not affected by scaling.

1) *Stability of the cosine against scaling:* For two vectors $u, v \in \mathcal{R}^d$, the cosine between is defined as:

$$\cos(u, v) = \frac{u \cdot v}{\|u\| \|v\|} = \frac{\sum_{i=0}^d u_i v_i}{\sqrt{\sum_{i=0}^d u_i^2} \sqrt{\sum_{i=0}^d v_i^2}} \quad (13)$$

Therefore, it follows that scaling one vector with a scaling factor $\lambda \neq 0$ does not affect the cosine as:

$$\cos(\lambda u, v) = \frac{\sum_{i=0}^d (\lambda u_i) v_i}{\sqrt{\sum_{i=0}^d (\lambda u_i)^2} \sqrt{\sum_{i=0}^d v_i^2}} = \frac{\lambda \sum_{i=0}^d u_i v_i}{\lambda \|u\| \|v\|} = \cos(u, v) \quad (14)$$

2) *Proof of theorem 1:* Let $W_{t,k}^*$ be the poisoned model of client k in round t , G_t the respective global model, $U_{t,k}^* = W_{t,k}^* - G_t$ the update, $\gamma_{t,k} \neq 0$ an arbitrary scaling factor unequal 0 (cf. Eq. 3). For simplicity, $C_{t,k,i}^*$ denotes the NEUP

TABLE VII: Main Task Accuracy (MA), Backdoor accuracy (BA), Poisoned Probability (PRC) and Benign Probability (NPV) of DeepSight for different NLP backdoors.

Trigger sentence	Backdoor	No Defense		DeepSight			
		BA	MA	BA	MA	PRC	NPV
"search online using"	"bing"	100.0	22.5	0.0	22.6	100.0	100.0
"barbershop on the corner is"	"expensive"	100.0	22.2	0.0	22.6	100.0	100.0
"pasta from astoria tastes"	"delicious"	100.0	22.4	0.0	22.6	100.0	100.0
"adore my old"	"nokia"	100.0	22.5	0.0	22.6	100.0	100.0
"my headphones from bose"	"rule"	100.0	22.3	0.0	22.6	100.0	100.0
	Average	100.0	22.3	0.0	22.6	100.0	100.0

TABLE VIII: Effectiveness of DeepSight for the CIFAR-10 dataset, if each local dataset contains only samples with a single label. All values in percentage

Defense	BA	MA	PRC	NPV
No Attack	0.0	92.2	-	-
No Defense	100.0	76.6	-	-
DeepSight	0.0	91.9	-	80

for the neuron i of the scaled model $W'_{t,i}$, $C_{t,k,i}$ of the unscaled model $W_{t,k}^*$ and analogously for the energy $\mathcal{E}_{t,k,i}^*$ as well as the update of bias of neuron i for client k in round t $b_{t,k,i}^u$. Therefore, the following relation holds:

$$b_{t,k,i}^* = \lambda_{t,k} b_{t,k,i}^u + b_{t,G_t,i} \quad (15)$$

and analogously for the individual weight updates $w_{t,k,i,h}^u$. Therefore, $C_{t,k,i}^* = C_{t,k,i}$ holds:

$$\begin{aligned} C_{t,k,i}^* &= \frac{\mathcal{E}_{t,k,i}^{*2}}{\sum_{j=0}^P \mathcal{E}_{t,k,j}^{*2}} \\ &= \frac{\left(|b_{t,k,i}^* - b_{t,G_t,i}| + \sum_{h=0}^H |w_{t,k,i,h}^* - w_{t,G_t,i,h}| \right)^2}{\sum_{j=0}^P \left(|b_{t,k,j}^* - b_{t,G_t,j}| + \sum_{h=0}^H |w_{t,k,j,h}^* - w_{t,G_t,j,h}| \right)^2} \\ &= \frac{\left(|\lambda_{t,k} b_{t,k,i}^u + b_{t,G_t,i} - b_{t,G_t,i}| + \sum_{h=0}^H |w_{t,k,i,h}^u - w_{t,G_t,i,h}| \right)^2}{\sum_{j=0}^P \left(|\lambda_{t,k} b_{t,k,j}^u + b_{t,G_t,j} - b_{t,G_t,j}| + \sum_{h=0}^H |w_{t,k,j,h}^u - w_{t,G_t,j,h}| \right)^2} \\ &= \frac{\left(|\lambda_{t,k} b_{t,k,i}^u| + \sum_{h=0}^H |\lambda_{t,k} w_{t,k,i,h}^u + w_{t,G_t,i,h} - w_{t,G_t,i,h}| \right)^2}{\sum_{j=0}^P \left(|\lambda_{t,k} b_{t,k,j}^u| + \sum_{h=0}^H |\lambda_{t,k} w_{t,k,j,h}^u + w_{t,G_t,j,h} - w_{t,G_t,j,h}| \right)^2} \\ &= \frac{\left(|\lambda_{t,k} b_{t,k,i}^u| + \sum_{h=0}^H |\lambda_{t,k} w_{t,k,i,h}^u| \right)^2}{\sum_{j=0}^P \left(|\lambda_{t,k} b_{t,k,j}^u| + \sum_{h=0}^H |\lambda_{t,k} w_{t,k,j,h}^u| \right)^2} \\ &= \frac{\lambda_{t,k}^2 \left(|b_{t,k,i} - b_{t,G_t,i}| + \sum_{h=0}^H |w_{t,k,i,h}^* - w_{t,G_t,i,h}| \right)^2}{\lambda_{t,k}^2 \sum_{j=0}^P \left(|b_{t,k,j} - b_{t,G_t,j}| + \sum_{h=0}^H |w_{t,k,j,h}^* - w_{t,G_t,j,h}| \right)^2} \\ &= \frac{\lambda_{t,k}^2 \mathcal{E}_{t,k,i}^{*2}}{\lambda_{t,k}^2 \sum_{j=0}^P \mathcal{E}_{t,k,j}^{*2}} = C_{t,k,i} \quad \square \end{aligned}$$

I. Impact of Threshold Factor

The boundary for the Threshold Exceedings $\xi_{t,k}$ of a client k in round t is determined by multiplying the highest NEUP $C_{t,k,\max}$ (cf. Eq.9) for this model with a threshold factor (TF) of 1 % but at most $1/P$, where P is the number of labels of the respective data scenario (cf. Eq.10). In the following, we discuss the impact of TF on DeepSight's performance.

Reducing the Threshold Factor (TF) decreases $\xi_{t,k}$ for all clients. This will increase the Threshold Exceedings (TEs) for all clients, as more NEUPs of a model will be above the threshold $\xi_{t,k}$. Since many NEUPs of benign models are already above the threshold, especially the TE's of poisoned models are increased, making them less suspicious during the classification, increasing the false-negative rate (FNR).

We conducted an experiment on the IoT-Traffic dataset to confirm this analysis. Figure 8 shows the number of Threshold Exceedings averaged over 70 benign models (green line), 30 malicious models (red line), the resulting classification boundary (blue line) for different TFs. Further, it shows the TPR (dashed red line) and FPR (dashed green line) when applying the classification boundary and marks the TF of DeepSight in black. As Fig. 8 shows, when the TF is reduced, the TPR is reduced.

On the other side, increasing TF reduces analogously the TE's, especially for benign models, increasing the number of

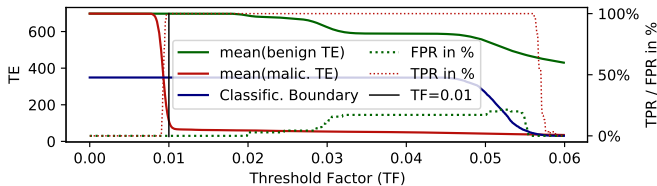


Fig. 8: Average number of benign Threshold Exceedings (mean(benign TE)), average number of malicious Threshold Exceedings (mean(malic. TE)), Classification boundary, FPR, and TPR for different Threshold Factors (TF).

false positives. If many benign models are affected, then the classification boundary will also be moved, s.t. the TEs for poisoned models are below this boundary, increasing the FNR. This is also visible in Fig. 8, as first the FPR grows and at some point, if the $TF > 0.05$, the classification boundary is moved, s.t. first the FPR is reduced and then the TPR.

J. Overhead and Complexity of DeepSight

The computational effort of DeepSight depends on the number of parameters M and number of models N . For the IoT-Traffic ($N=100$ models, $M=300k$) DeepSight requires 1.15 minutes and 1.06 minutes for CIFAR-10 ($N=10$ models, $M=9M$) to perform filtering and aggregating the remaining, clipped models. With Reddit ($M=20M$, $N=100$ models; 6.02 minutes), DeepSight was evaluated also on large-scale models. Although, the pairwise distance matrices grow with complexity $\mathcal{O}(n^2)$, calculating pairwise distances took less than 1s for the NLP setting. Only calculating the DDifs required a higher amount of time (5.7 minutes for NLP models). However, computing DDifs scales with $\mathcal{O}(N)$. Furthermore, the experimental code was not parallelized. Since DDifs for different models and different seeds are independent they can be calculated in parallel, reducing the time by a factor of 300.

K. Ablation Study of DeepSight’s Components

Table IX shows the effectiveness, i.e., the ratio of filtered poisoned models to the total number of poisoned models (TPR), of different defenses that are based on DeepSight’s individual components for different corner cases. The clustering defenses realize outlier detection-based filtering schemes, using the proposed techniques, while the classifier is based only on the Threshold Exceedings, without any further support. As the table shows, the cosine and DDif clustering are weakened in some corner cases, e.g., if the learning rate is too low or the anomaly evasion loss function uses the DDifs. Also the Threshold Exceedings classifier is weakened in few cases, e.g., when multiple backdoors are injected or when the adversary \mathcal{A} uses a low PDR.

On the other side, DeepSight always detects all poisoned models, as it combines all individual techniques, s.t. they can compensate each others’ weak spots. Also the classifier profits from the clusterings, as this allows to use the labels of similar models (cf. §V-A4).

It should be noted, that for the NLP scenario, the outlier-detection defense that uses DDifs is completely circumvented. This is caused by the highly non-IID nature of this scenario, s.t. the benign models differ significantly, while the poisoned models are very similar to each other. Therefore, the clustering considers them as the majority and all other (benign) models as outliers. This demonstrates the advantage of using clustering only for identifying similar model updates, as it is done in

TABLE IX: TPRs of defenses that are based on DeepSight’s components for different PDRs, different factors for a DDif based anomaly evasion function (α), number of epochs of the malicious client (#epochs), learning rate for the malicious clients (lr), PMRs, starting from a randomly initialized model (random), three different backdoors ($BC = 3$), a combination of different techniques (Sophisticated: $PMR = 40\%$, DDif based loss function, $\alpha = 0.1$, #epochs = 3, $PDR = 20\%$), as well as the normal NLP scenario (default) and 4 times reduced PDR (reduced PDR).

FL Appl.	Device Type	Scenario	Cosine Clust.	DDif Clust.	NEUP Clust.	NEUP Classifier	DeepSight
NIDS	Netatmo Weather	PDR = 10 %	100.0	63.3	100.0	60.0	100.0
		PDR = 50 %	100.0	100.0	100.0	100.0	100.0
		PDR = 80 %	100.0	100.0	100.0	100.0	100.0
		$\alpha = 0.1$	100.0	0.0	100.0	100.0	100.0
		#epochs = 1	100.0	100.0	100.0	100.0	100.0
		#epochs = 15	100.0	100.0	100.0	100.0	100.0
		$lr = 10^{-4.5}$	100.0	0.0	100.0	100.0	100.0
		$lr = 10^{-2.0}$	100.0	100.0	100.0	100.0	100.0
		PMR = 45 %	100.0	100.0	100.0	100.0	100.0
		random model	100.0	100.0	100.0	100.0	100.0
		BC = 3	100.0	100.0	100.0	68.0	100.0
		Sophisticated	100.0	20.0	100.0	100.0	100.0
Edimax Plug	Netatmo Cam	PDR = 10 %	0.0	100.0	100.0	36.7	100.0
		PDR = 50 %	100.0	96.7	100.0	63.3	100.0
		PDR = 80 %	100.0	100.0	100.0	100.0	100.0
		PDR = 10 %	16.7	100.0	100.0	50.0	100.0
		PDR = 50 %	100.0	56.7	100.0	63.3	100.0
		PDR = 80 %	100.0	80.0	100.0	100.0	100.0
NLP		default	100.0	0.0	100.0	100.0	100.0
		reduced PDR	100.0	0.0	100.0	100.0	100.0

DeepSight, and the negative impact of using clustering-based techniques as a classifier.

L. Backdoor Detection in Centralized Settings

Liu *et al.* propose an orthogonal approach for centralized learning that aims to detect trojaned Neural Networks (NN), where the backdoor is activated by a trigger patch in the image. They assume that the poisoned dataset consists of benign images and the adversary \mathcal{A} puts a colored patch on those images to create triggered versions of them, s.t. the dataset contains the same image multiple times, without trigger and correct label and with trigger and backdoor target as label. They assume that this causes a neuron in the later layers to being trained to determine the presence of the trigger and, if activated, overrules all other neurons in the same layer. They use benign input data to determine a valid output state for the second last layer, consisting of the activation status for each neuron. Their approach then changes the activation status of each neuron while observing the probabilities that the NN predicts. A model is considered as trojaned if a single neuron changes the output of the NN significantly [17]. However, even if this approach works for patch triggers, for semantic backdoors the trigger can consist of the whole input, s.t. their basic assumption does not hold. DeepSight considers also semantic backdoors, where the trigger is, e.g., the color of the car for image datasets [2] or in case of the NIDS scenario the whole packet sequence [27]. Therefore, those backdoors are not activated by a small fraction of the input features but depend on the whole input, preventing that the dataset can contain a sample multiple times and making it less likely that a single neuron is responsible for activating the backdoor. Moreover, it is not possible to classify behavior statically as malicious as this depends on the behavior of the benign clients. Finally, the assumption that the server has validation data is not practical (cf. §III-C).